Nano Trends 3 (2023) 100013

Contents lists available at ScienceDirect

Nano Trends

journal homepage: www.elsevier.com/locate/nantre

Development and application of nanogenerators in humanoid robotics

Xuecheng Qu [a,b], Ze Yang [a], Jia Cheng [a,*], Zhou Li [b,c,*], Linhong Ji [a,*]

[a] State Key Laboratory of Tribology in Advanced Equipment, Department of Mechanical Engineering, Tsinghua University, Beijing, 100084, China
[b] CAS Center for Excellence in Nanoscience, Beijing Key Laboratory of Micro-nano Energy and Sensor, Beijing Institute of Nonenergy and Nanosystems, Chinese Academy of Sciences, Beijing, 101400, China
[c] School of Nanoscience and Technology, University of Chinese Academy of Sciences, Beijing 100049, China

ARTICLE INFO

Keywords:
Nanogenerator
Humanoid sensor
Robotics
Soft finger
Human-machine interaction

ABSTRACT

Nanogenerators have garnered significant attention in the field of robotics due to their high performance, ease of design and fabrication, and lightweight nature. By utilizing such sensing systems, machines can be endowed with specific sentience capabilities. Moreover, sensors that based on nanogenerators can operate continuously without requiring an external power source. The following paper presents a comprehensive review of recent developments and applications of nanogenerator-based sensors in robotics in recent years. These sensors are categorized according to their sensory functions (including tactile, hearing, smell, vision and displacement, etc.), with a focus on their working mechanisms, materials and structures. Furthermore, this review investigates the usage of these devices in flexible manipulators and human-machine interfaces. Finally, the challenges and opportunities pertaining to nanogenerator-based sensors are discussed.

1. Introduction

In the new generation of technological revolution, the development of sensing technology is a crucial aspect of information acquisition [1,2]. It plays an important role for robots in the autonomous behavior, remote observation, and interaction capabilities in special environments [3,4]. However, traditional sensors may not suffice to meet robots' application requirements in complex and variable environments. For example, while visual sensors can enable robots to approximate their environment, they cannot sense gripping force information visually [5]. Therefore, to improve intelligent robots' perception accuracy and intelligence, it is necessary to further enhance the performance and functionality of sensors [6,7].

The various natural sensory systems of living organisms work in unique ways and demonstrate remarkable performance, providing rich inspiration for sensor systems [8–10]. Recently, remarkable progress has been made in developing novel sensing technologies that can mimic human sensory systems through biomimetics [11–13]. This progress has led to the creation of innovative electronic systems with the potential to create humanoid robots with finely tuned sensory capabilities, similar to our own [9,14]. Novel sensor systems expand robots' perception capabilities, and significant progress in the field of nanomaterials and micro-nanomanufacturing accelerate the development of flexible electronics products, especially tactile sensors that give robots the ability to perceive more subtle touch-based information from environment [15,16]. The collaborative operation of flexible tactile sensors and flexible mechanical hands enable robots to perform expected tasks more accurately [17–25]. Electronic ears and noses can give robots the ability to perceive rich environmental information such as sound and gasses [26–30]. Additionally, angle and displacement sensors play a vital role in robots' perception of complex environments and enhance their autonomous behavior [31–35].

The diversification, intellectualization, and interdisciplinary nature of humanoid sensory systems have also greatly promoted the development of human-machine interaction (HMI) [36–41]. The ultimate goal of this field is to make interactions with machines as natural as human-to-human interactions [42–44]. However, intelligent robots require sufficient performance and long-term stable operation to realize specific functions [45]. Therefore, it is crucial that sensing systems operate with minimal power consumption [46]. Ideally, these sensors should be self-powered. Recently, the development of self-powered sensing devices with high performance, versatile features, and integration capabilities with complex electronic devices has become a research hotspot in this field [46,47]. Piezoelectric nanogenerators (PENGs) [48] and triboelectric nanogenerators (TENGs) [49] have recently been proven to be novel and effective mechanical-to-electrical signal conversion methods, which can serve as the foundation for self-powered sensor research and provide technical support for achieving high performance, new functions, and expanding into new application areas [50–78]. This review delves into the most recent developments in nanogenerator-based sensors for

* Corresponding authors.
E-mail addresses: chengjia@tsinghua.edu.cn (J. Cheng), zli@binn.cas.cn (Z. Li), jilh@tsinghua.edu.cn (L. Ji).

https://doi.org/10.1016/j.nwnano.2023.100013
Received 26 May 2023; Received in revised form 20 June 2023; Accepted 20 June 2023

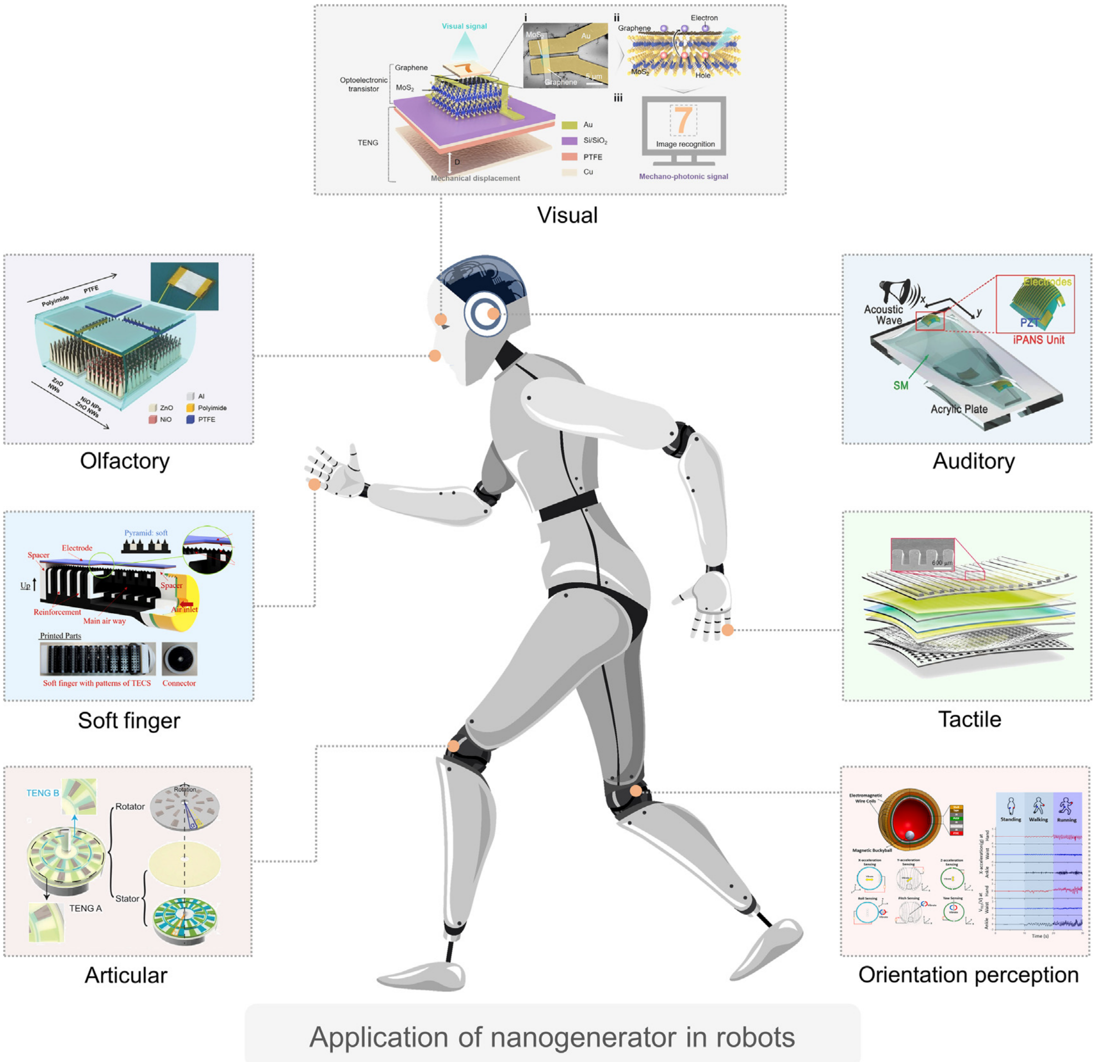

Fig. 1. Current state-of-the-art piezoelectric nanogenerator and triboelectric nanogenerator technologies and their applications for robotics. (For interpretation of the references to color in this figure legend, the reader is referred to the web version of this article.)

human-robot interaction, with a focus on their applications in various humanoid functions including tactile, hearing, smell, vision and displacement, etc. (Fig. 1) [59]. We've explored how these sensors impact different aspects of people's lives and discussed the challenges faced by the field. Additionally, we've provided insights into potential future advancements in this area.

2. Working mechanism of nanogenerator

Nanogenerator is a device that converts mechanical energy into electrical energy by driving displacement currents in the Maxwell equation [79]. To homogeneous dielectrics, $P = (\varepsilon - \varepsilon_0)E$, $D = \varepsilon E$. Note that P is the polarization field density, ε stands for the permittivity of a dielectric, ε_0 is the vacuum permittivity, D is the displacement field. So that Maxwell displacement current [80]:

$$J_D = \frac{\partial D}{\partial t} = \varepsilon_0 \frac{\partial E}{\partial t} + \frac{\partial P}{\partial t} \tag{1}$$

Considering the existence of polarization charge in the dielectric, such as triboelectric materials and piezoelectric materials, there exists polarization charge density P_S which caused by surface static charge in displacement current:

$$J_D = \frac{\partial D}{\partial t} = \varepsilon_0 \frac{\partial E}{\partial t} + \frac{\partial P_S}{\partial t} \tag{2}$$

Note that, the first term on the right side of the equation is the current generated by the changing electric field, and the second term is the current caused by the polarization field generated by the electrostatic charge on the surface, which is the fundamental source and theoretical basis of the nanogenerator.

2.1. Working mechanism of TENG

The working mechanism of TENG is based on the coupling effect between triboelectric and electrostatic induction [81]. Take the contact separation model for example, when two materials of different polarity come into contact, charge transfer will occur due to the different binding capacity of the materials for electrons. The electrostatic field established by the triboelectric charge drives the flow of electrons through the external load, resulting in the accumulation of free electrons $\sigma_1(z,t)$ in the electrode [70]. The electric field of two dielectric with dielectric constant and thickness of ε_1, ε_2 and d_1, d_2 are $E_z = \sigma_1(z,\ t)/\varepsilon_1$ and $E_z = \sigma_1(z,\ t)/\varepsilon_2$, respectively. The electric field at the gap $E_z = (\sigma_1(z,\ t) - \sigma_c) - \varepsilon_0$. The relative voltage difference between two electrodes:

$$V = \sigma_1(z,\ t)\left[\frac{d_1}{\varepsilon_1} + \frac{d_2}{\varepsilon_2}\right] + \frac{Z\left[\sigma_1(z,\ t) - \sigma_c\right]}{\varepsilon_0} \tag{3}$$

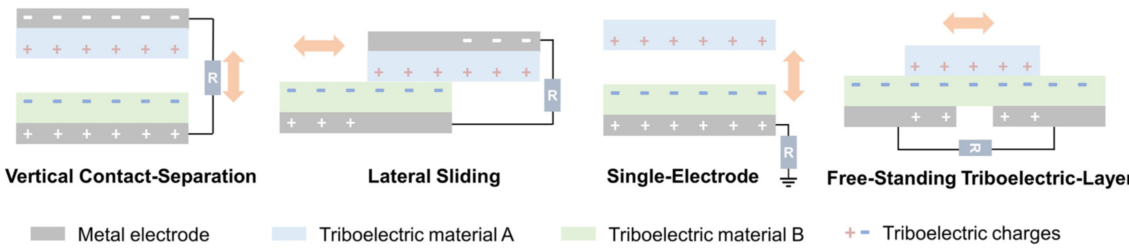

Fig. 2. Four fundamental modes of triboelectric nanogenerators. (For interpretation of the references to color in this figure legend, the reader is referred to the web version of this article.)

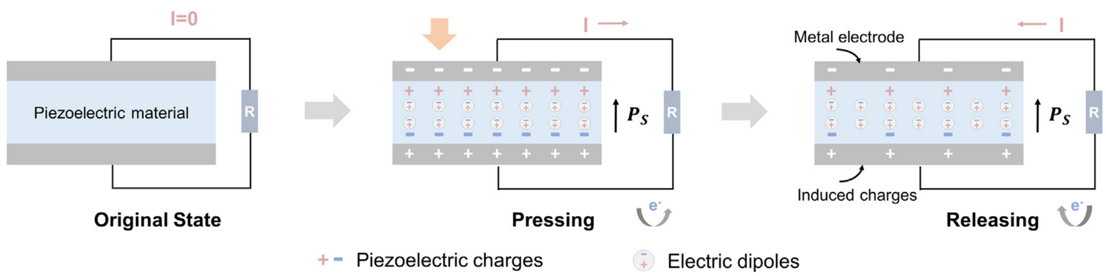

Fig. 3. Working mechanism of piezoelectric nanogenerator. (For interpretation of the references to color in this figure legend, the reader is referred to the web version of this article.)

Due to the existence of external load resistance R, according to Ohm's law, the external output current density:

$$RA\frac{d\sigma_1(z,\ t)}{dt} = \frac{z\sigma_c}{\varepsilon_0} - \sigma_1(z,\ t)\left[\frac{d_1}{\varepsilon_1} + \frac{d_2}{\varepsilon_2} + \frac{d_3}{\varepsilon_3}\right] \tag{4}$$

Where z depends on the function t of the dynamic process of applying force, and A is the area of the electrode.

The researchers have identified four primary working modes for the TENGs, which include vertical contact-separation mode, lateral sliding mode, single-electrode mode, and freestanding triboelectric-layer mode (Fig. 2). These fundamental modes serve as the foundation for all TENG structures, and are adaptable to various applications by deriving different structures [82].

2.2. Working mechanism of PENG

Piezoelectricity is a phenomenon where there is a coupling between stress and strain tensors, electric displacement and electric field vectors, and elastic and dielectric variables [83]. In anisotropic piezoelectric materials, the centers of positive and negative charges coincide in the initial state. When external stresses are applied to cause deformation, the charge centers of anions and cations will separate, leading to potential differences (Fig. 3). The general coupled equations in terms of piezoelectric strain-charge form as [84]:

$$\{D\} = \left[\varepsilon^T\right]\{E\} + [d]\{T\} \tag{5}$$

$$\{S\} = \left[S^E\right]\{T\} + \left[d^t\right]\{E\} \tag{6}$$

Where $[d]$ is the matrix of the direct piezoelectric effect, d^t is the matrix used to describe the indirect piezoelectric effect. T and E indicate a zero (or constant) stress and electric fields, respectively, from the system. t defines the transposition of the matrix.

The open circuit voltage of PENG is $V_{OC} = z\sigma_P(z)/\varepsilon$. Due to the existence of external load resistance R, according to Ohm's law, the external output current density:

$$RA\frac{d\sigma}{dt} = \frac{z\left[\sigma_P(z) - \sigma(t)\right]}{\varepsilon} \tag{7}$$

3. Application of nanogenerator in humanoid robotics perception

3.1. Electronic skin/tactile simulation

Electronic skin/tactile sensors are consistently fundamental and indispensable components in the realm of intelligent robots [85]. Electronic skin/tactile sensors are electronic devices that can detect external mechanical stimuli (such as strain, pressure, humidity, and temperature) and quantify the relevant information into electrical signals, mimicking the perceptual function of human skin [25,86]. Researchers are continuously exploring and optimizing materials, physical structures, processing techniques, etc., in order to improve the resolution, sensitivity, detection range, functional diversity, and lifespan of tactile sensors [86,87].

Tactile sensors based on nanogenerators can detect and respond to external environmental stimuli without the need for an external power source, which could detect physical phenomena such as pressure distribution, strain, shear force, and sliding [17,18,88]. These self-powered tactile sensors have already found initial applications in the field of intelligent robotics. In this section, we will mainly introduce several typical functional tactile sensors based on nanogenerators.

A selective sensitivity of tactile sensing to pressure and vibration is critical for mimicking the skin of a human. In 2019, Chun et al. proposed an innovative self-powered flexible neural tactile sensor (NTS) that demonstrated the ability to detect pressure and recognize fine textures, which was composed of interlocked percolative graphene sensor (bottom panel) and TENG sensor (top panel) with fingerprint-inspired periodic microlines (Fig. 4a) [89]. The output signals of this device were similar to the real output signal produced by the slow adaptive (SA) and fast adaptive (FA) mechanoreceptors in human skin. In 2022, Kim et al. proposed self-powered multifunctional ionic tactile sensor (SMITS), which composed of a single-electrode triboelectric nanogenerator (SETENG) and a capacitive ionic sensor (CIS) with poly (vinylidene fluoride-trifluoroethylene) (P(VDF55-TrFE45)) nanofibers (NFs) (Fig. 4b). The SETENG was designed laminated on top of the CIS, with both components sharing a common electrode (AgNW/PDMS). This device could measure pressures ranging from 0 to 60 kPa and temperatures ranging from 25° to 45 °C without requiring any additional energy supply [90].

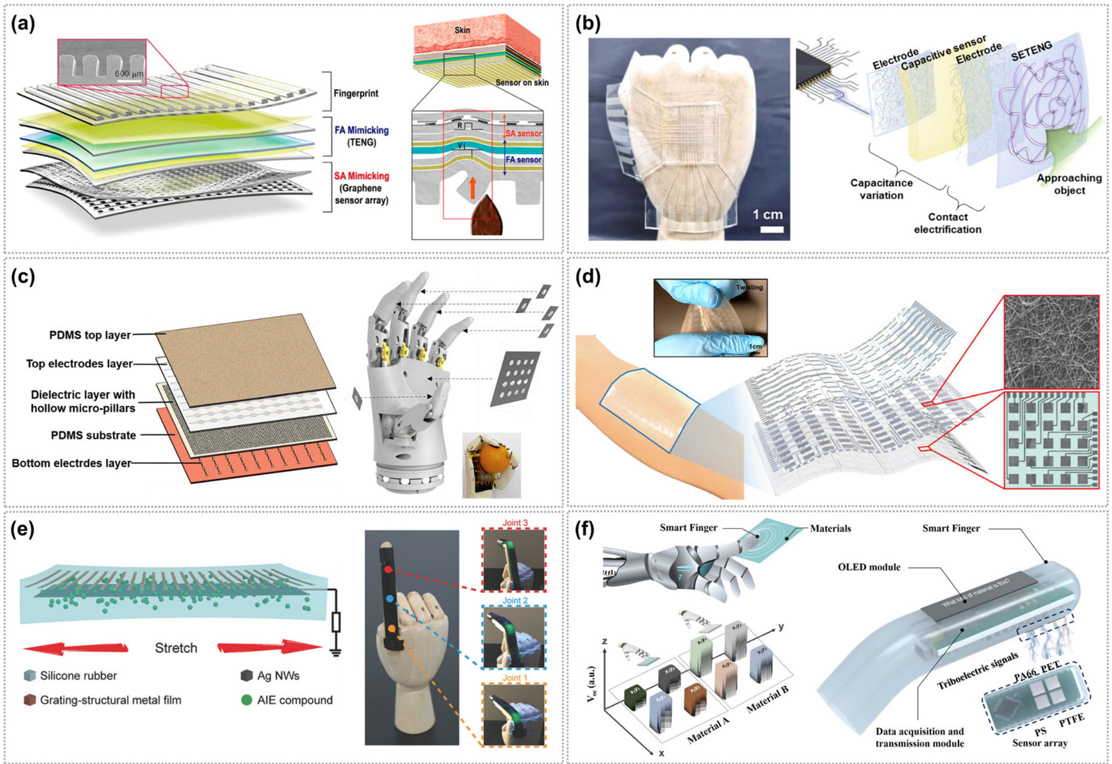

Fig. 4. Nanogenerator-based electronic skin/tactile sensors. (a) Flexible neural tactile sensor (NTS) to detect pressure and recognize fine textures [89]. Copyright (2019) by American Chemical Society. (b) Self-powered multifunctional ionic tactile sensor (SMITS) to measure pressure and temperature [91]. Copyright (2022) by Elsevier. (c) Stretchable dual-mode sensor to scan object shape, measure grasping pressure and detect object hardness [92]. Copyright (2019) by Elsevier. (d) Flexible TENG based sensor array [93]. Copyright (2022) by Elsevier. (e) Stretchable triboelectric–photonic smart skin (STPS) to convert pressure information into optical information [94]. Copyright (2018) by John Wiley and Sons. (f) Artificial tactile perception smart finger to identify material type and roughness [95]. Copyright (2022) by AAAS. (For interpretation of the references to color in this figure legend, the reader is referred to the web version of this article.)

However, sensors based on planar structures may have certain limitations in terms of mechanical properties and the range of functions they can perform. In order to overcome this difficulty, in 2019, Han et al. presented a controlled, nonlinear buckling process for creating intricate 3D piezoelectric (polyvinylidene difluoride, PVDF) microsystems with improved responsivity (anisotropic responses and sensitivity of 60 mV N^{-1} for normal force) from lithographically defined two-dimensional patterns of electrodes and thin films of piezoelectric polymers [91]. These 3D piezoelectric systems were well configured and mounted on the manipulator for interactions with environment in three dimensions to distinguish the direction/position of mechanical stimuli such as pressure, normal force, stretching and bending.

In 2019, Zhang et al. created a stretchable dual-mode sensor, consisting of cross-grid liquid metal electrode arrays separated by a microstructured dielectric layer (Fig. 4c) [92]. The combination of capacitive (10–120 kPa) and TENG (<10 kPa) modes expanded its pressure monitoring range and sensitivity (highest 1.04 V/kPa) for robots to scan object shape, measure grasping pressure and detect object hardness.

Generally speaking, the design of array electrodes will have certain signal crosstalk problems, which may limit the pixel density of the device. In 2023, Li et al. proposed a flexible TENG-based sensor array with high pixel density (100 sensing units within the overall size of 7.5 cm × 7.5 cm), that polydimethylsiloxane (PDMS) cast in each cell as the triboelectric layer for independent sensing (Fig. 4d) [93]. Each unit showed good sensitivity of 0.11 V/kPa with a wide range of pressure detection from 10 to 65 kPa, where the maximum crosstalk output is only 10.8%. And the pressure distribution of the object on the device can be displayed by software.

By using reversible aggregation-induced emission (AIE) compound bis (4-phenothiazine phenyl) sulfone as a solid intensive fluorescent emitter and a grating-structured metal film, in 2018, Bu et al. developed a stretchable triboelectric–photonic smart skin (STPS) as shown in Fig. 4e [94]. The device converts pressure information into optical information without the need for an external power source, showing abilities of tactile sensing and gesture interpretation.

At present, researchers are primarily focused on the utilization of tactile sensors in mechanical detection. While there have been significant advancements in this area, accurately quantifying material type information through tactile sensors remains a challenge. This bottleneck limits the interaction between intelligent robots and the environment. In 2022. Qu et al. developed an artificial tactile perception smart finger based on the triboelectric effect between materials and sensors with four typical materials (Polyamide, PA66; Polyethylene terephthalate, PET; Polystyrene, PS; Polytetrafluoroethylene, PTFE), which quantified tactile psychological parameters to realize widely applicable material type and roughness identification (Fig. 4f) [95]. The recognition accuracy rate was as high as 96.8% under the synergy of machine learning. This tactile technology based on triboelectric sensing enables robotic hands to have the ability to recognize materials, which has great potential in the fields of medical rehabilitation and intelligent industry.

3.2. Auditory simulation

The hearing system of a robot is crucial for its perception and serves as an effective way to establish direct communication between humans and robots. The majority of vocal energy is typically concentrated within the frequency range of 100 to 4000 Hz [96]. Traditional auditory sensors rely on microphones that integrate precise signals with processing circuits, which can lead to increased power consumption and shorter operating cycles [97]. Therefore, auditory sensors with low consumption, high sensitivity, wider frequency response and selectivity have

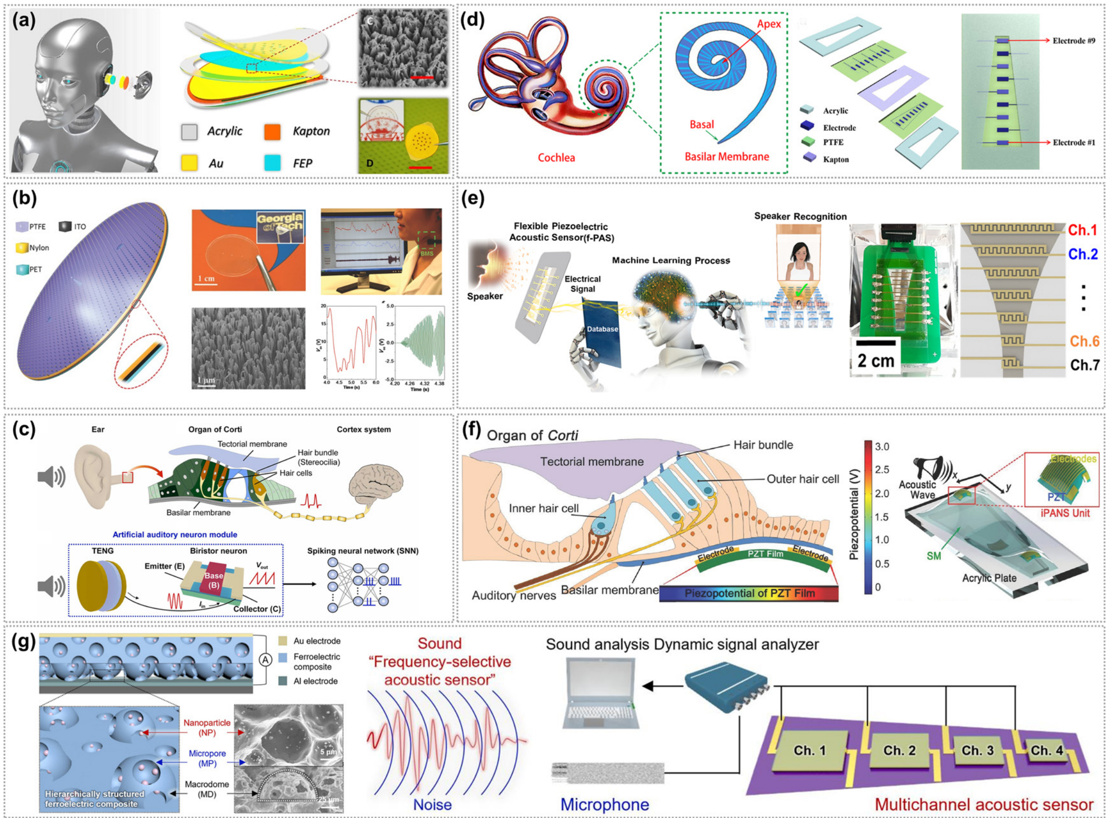

Fig. 5. Nanogenerator-based auditory sensors. (a) Triboelectric auditory sensor (TAS) for building an electronic hearing system (from 100 to 5000 Hz) [103]. Copyright (2018) by AAAS. (b) Bionic membrane sensor (BMS) inspired by the structure of eardrum to detect the broadband response of 0.1 to 3200 Hz [104]. Copyright (2015) by John Wiley and Sons. (c) Self-aware artificial auditory neuron module [105]. Copyright (2023) by Elsevier. (d) TENG-based device with nine channels (from 20 to 3000 Hz) [106]. Copyright (2018) by Springer Nature. (e) Piezoelectric acoustic sensor (f-PAS) with seven channels [107]. Copyright (2015) by Elsevier. (f) Inorganic piezoelectric acoustic nanosensor (iPANS) to mimic biomimetic basilar membrane [108]. Copyright (2014) by John Wiley and Sons. (g) Dual-mode device based on triboelectric technology with wide dynamic range of frequency selectivity (from 145 to 9000 Hz) [109]. Copyright (2022) by AAAS. (For interpretation of the references to color in this figure legend, the reader is referred to the web version of this article.)

the potential to address challenges related to social interaction and power/energy in robotics [98].

Recently, triboelectric and piezoelectric acoustic sensors based on mimicking the basilar membrane of the human cochlea have been considered as promising candidates for improving sensitivity and recognition rate, which have unique advantages in material selection and structural processing [99,100]. By providing accurate and selective auditory information, these sensors may lead to significant improvements in the overall performance and functionality of robotic systems, while reducing their reliance on external power sources [101,102]. In this section, we will mainly introduce the research progress of biomimetic nanogenerator-based acoustic sensors.

In 2018, Guo et al. report single-channel and self-powered triboelectric auditory sensor (TAS) for building an electronic hearing system for robotics, which showed good sensitivity (110 millivolts/decibel) and effective broadband response (from 100 to 5000 Hz) as shown in Fig. 5a [103]. One of the friction layers of fluorinated ethylene propylene (FEP) with several hole channels could be redesigned for selective frequency adjusting. In 2015, Yang et al. reported a bionic membrane sensor (BMS) inspired by the structure of eardrum could detect the broadband response of 0.1 to 3200 Hz with good broad dynamic range (51 mV Pa^{-1}, in a range of 2.5–1200 Pa) as shown in Fig. 5b [104]. These works can simplify the signal processing circuit and reduce the power consuming, expressing notable advantages of using TENG technology to build a new generation of auditory systems for robotics.

While the biomimetic auditory sensors mentioned earlier possess exceptional electrical properties, they do not yet form a full auditory system that mimics human hearing entirely. In 2023, Yun et al. proposed a self-aware artificial auditory neuron module, which was constructed by serially connecting a TENG (as auditory sensor and energy collector) and a bi-stable resistor (as spike neuron). The device could detect the sound pressure level and simultaneously encoded it into the form of a spike, which was used as an input neuron for the spike neural network (Fig. 5c) [105].

In contrast to the previous concepts, some researchers utilize a multichannel structure as the foundation for selecting sound frequency responses. In 2018, Liu et al. reported a TENG-based device that achieved a high degree of frequency selectivity, covering a range of 20 to 3000 Hz, by evenly placing nine silver electrodes on each of two polytetrafluoroethylene membranes in a trapezoidal pattern (Fig. 5d) [106]. In 2018, Han et al. proposed a flexible piezoelectric acoustic sensor (f-PAS) with seven channels of interdigitated electrodes patterned on the PZT membrane (Fig. 5e) [107]. The multichannel analysis was employed to selectively detect the resonance frequencies of each mode in the region where oscillatory motion was observed. The resonance frequency of the flexible piezoelectric membrane is described as following equation:

$$f_{\tau} = \frac{\omega}{2\pi} = C\frac{t}{l^2}\sqrt{\frac{E}{\rho}} \tag{8}$$

where ω are angular frequency of the trapezoidal membrane, C, t, E, and ρ indicate the capacitance, thickness, Young's modulus, width, and density of the film, respectively. Similarly, in 2014, Lee et al. reported an inorganic piezoelectric acoustic nanosensor (iPANS) by transferring PZT thin film onto trapezoidal silicone-based membrane (SM) to mimic

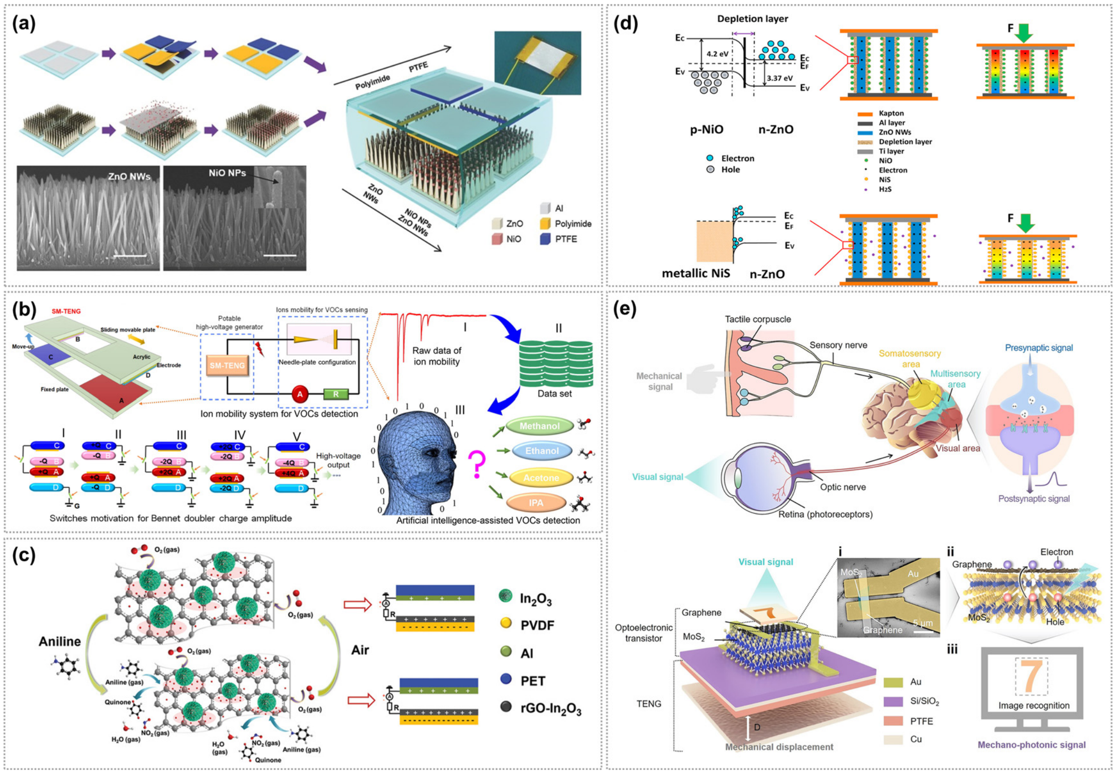

Fig. 6. Nanogenerator-based olfactory/visual sensors. (a) TENG-based olfactory sensor to distinguish four volatile organic compound (VOC) gasses (methanol, ethanol, acetone, and toluene) [110]. Copyright (2015) by John Wiley and Sons. (b) Machine learning (ML)-enhanced self-powered ion mobility strategy with a triboelectric-based ionizer [112]. Copyright (2021) by Elsevier. (c) TENG-based olfactory sensor with low-resistant rGO-In_2O_3 semiconductor to identify aniline-air gas [113]. Copyright (2020) by John Wiley and Sons. (d) PENG-based olfactory sensor with NiO/ZnO to identify H_2S gas [114]. Copyright (2016) by Elsevier. (e) Bioinspired mechano-photonic artificial synapse based on graphene/MoS_2 [115]. Copyright (2018) by Elsevier. (For interpretation of the references to color in this figure legend, the reader is referred to the web version of this article.)

biomimetic basilar membrane (BM), utilizing a laser lift-off technology to overcome the brittle characteristics of inorganic piezoelectric materials (Fig. 5f) [108]. Thanks to this stripping technique, vibration displacements of 7 nm to 17 nm could be detected with piezoelectric signals of 45 µV to 60 µV.

In 2022, Park et al. presented a dual-mode device contained frequency-selective acoustic and haptic sensors based on triboelectric technology, and featured a unique hierarchical structure consisting of ferroelectric composites with macrodome, micropore, and nanoparticle components (Fig. 5g) [109]. By adjusting shape factors like thickness and area of ferroelectric composites, it's possible to significantly enhance the dynamic range of frequency selectivity, which typically spans from 145 to 9000 Hz. Using machine learning techniques based on artificial neural networks (ANNs), the proposed device could achieve higher accuracy and selectivity than a commercial microphone, which has certain advantage in the field of robot audition.

3.3. Olfactory/visual simulation

Human nose contains approximately 400 olfactory receptors (OR). These receptors comprise a sophisticated network of multiple scent sensors, working together to identify and distinguish various odors. Several teams have developed electrochemical sensors, commonly referred to as electronic noses, that are capable of replicating the olfactory function of humans [110,111]. These electronic noses have proven to be effective in detecting gasses in robotic application [112]. Undoubtedly, one of the major hurdles in deploying portable sensor networks is the constraint posed by power limitations caused by high energy consumption rates and prolonged detection times. In response, some researchers have developed gas sensors based on self-powered technology.

In addition, research in the fields of neuroscience and cognitive psychology has revealed that over 80% of external information is processed by the brain through the sense of sight. While the digital camera has proven to be a successful electronic device that mimics the eye, it falls short in fully integrating all of the key features of the human visual system [11]. In this section, we will conduct a material-focused review of gas sensors and visual sensing systems that based on the nanogenerators.

In 2015, Kim et al. reported a self-powered sensing strategy that demonstrates highly selective gas detection capabilities, which could distinguish between four volatile organic compound (VOC) gasses (methanol, ethanol, acetone, and toluene) with a detection limit of 0.1% (Fig. 6a) [113]. The strategy was based on the physical contact between semiconducting nanowires (ZnO) and dielectric layers, which resulted in triboelectrification, as well as the heterogeneous catalytic reaction that took place on both the nanowires and nickel oxide (NiO) nanoparticles.

The ion migration phenomenon of plasma discharge satisfies the requirements of rapid gas detection. Based on the sensing mechanism of ion migration rate drift time, it can effectively identify various types of VOCs and their concentrations [114]. Based on this mechanism, in 2021, Zhu et al. proposed a machine learning (ML)-enhanced self-powered ion mobility strategy with a triboelectric-based ionizer (Fig. 6b) [115]. With ML algorithms, the specific features automatically from ion mobility spectrometry data was extracted, which had the characteristics of rapid response and low power consumption. In 2020, Chang et al. synthesized low-resistant rGO-In_2O_3 semiconductor composite using as the electrode of TENG, that the resistance was sensitive to aniline-air gas (Fig. 6c) [116]. When the rGO-In_2O_3 composite came into contact with an aniline-air gas mixture, the aniline molecules reacted with the absorbed oxygen species, resulting in the capture of electrons from the composites with its resistance decreases. Coupling effect of the

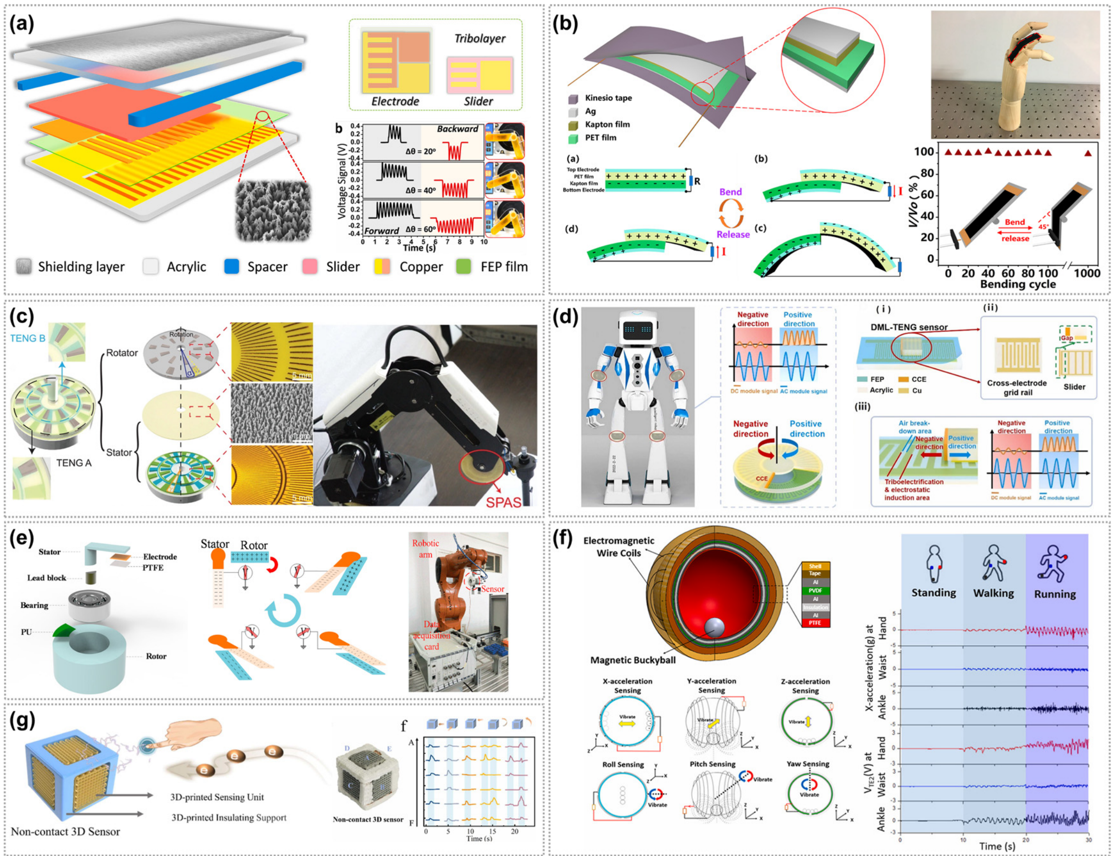

Fig. 7. Nanogenerator-based vector motion sensors. (a) Joint motion triboelectric quantification sensor (jmTQS) to detect the degree and speed of flexion/extension movements in fingers [122]. Copyright (2023) by Elsevier. (b) TENG-based stretchable sensor to detect motion and angle information [123]. Copyright (2018) by MDPI. (c) Rotating grating-structured self-powered angle sensor based on TENG [124]. Copyright (2023) by John Wiley and Sons. (d) Vector motion sensor based on dual-mode TENG to judge movement direction and angle [121]. Copyright (2023) by Elsevier. (e) TENG-based non-contact sensor to detect rotational movement [125]. Copyright (2020) by MDPI. (f) 3D activity inertial sensor (3DAIS) based on electromagnetic, piezoelectric, and triboelectric technologies [126]. Copyright (2023) by Elsevier. (g) CNF/MXene-based deep-trap hierarchical architecture for high-performance TENG [127]. Copyright (2023) by Elsevier. (For interpretation of the references to color in this figure legend, the reader is referred to the web version of this article.)

piezoelectric screening effect of ZnO and conversion of NiO/ZnO PN-junctions, in 2016, Qu et al. introduced heterogeneous structures into PENG and reported a self-powered H_2S gas sensor with high sensitivity of 0.49 (Fig. 6d) [117]. The self-powered electronic noses can simulate the human ability to perceive chemical substances in the external environment and does not require an external power supply. Future research directions include improving the sensitivity and selectivity of the sensors, as well as exploring more self-powered sensor materials and fabrication processes to further promote the practical applications of self-powered electronic noses.

In the self-powered visual sensing systems aspect. In 2021, Yu et al. presented a bioinspired mechano-photonic artificial synapse, which was composed of an optoelectronic transistor based on graphene/MoS_2 heterostructure and an integrated triboelectric nanogenerator (Fig. 6e) [118]. The triboelectric potential was utilized to operate the synaptic transistor and regulated the transfer or exchange of charges in the heterostructure, enabling the characteristic functions of a photonic synapse such as postsynaptic photocurrents, persistent photoconductivity, and photosensitivity. This work may emulate complex biological nervous system.

3.4. Vector motion sensors

Apart from the sensors mentioned above, vector motion sensors are essential for a robot to perceive and interact with environment. These sensors can detect linear and rotational displacement and provide information on dynamic acceleration in the direction of displacement [119,120]. Motion vector sensors with high precision recognition abilities are particularly important for obtaining motion parameters required to ensure accurate operation of the robot's automatic control system. TENG-based vector motion sensors generally adopt lateral sliding mode or freestanding triboelectric-layer mode [121]. PENG-based sensors, which are primarily used for monitoring vibrations at the nanometer/micrometer level, are not discussed in this section.

Most researchers use finger insertion electrodes or similar structures to measure displacement or angle information. The two contact layers are arranged in a regular pattern. As the contact layers come closer to each other, the metal layer surrounding them induces an electric potential, which is caused by electrostatic induction. Conversely, when the two contact layers move away from each other, a reverse potential is created.

In 2018, Pu et al. developed a sensor called the joint motion triboelectric quantification sensor (jmTQS), which utilized a grating structure to detect the degree and speed of flexion/extension movements in fingers (Fig. 7a) [122]. The sensor worked by counting the positive/negative pulses generated within a given time period. By analyzing the polarity of the coupling signal, the direction of rotation can be determined. With a similar structure, in 2018, Wang et al. described a stretchable motion sensor that utilized kinesio-tape and relied on the lateral sliding mode TENG to achieve the detection of motion and angle information (Fig. 7b) [123]. The stretched displacements and bending angles showed a strong linear correlation with both the short-circuit

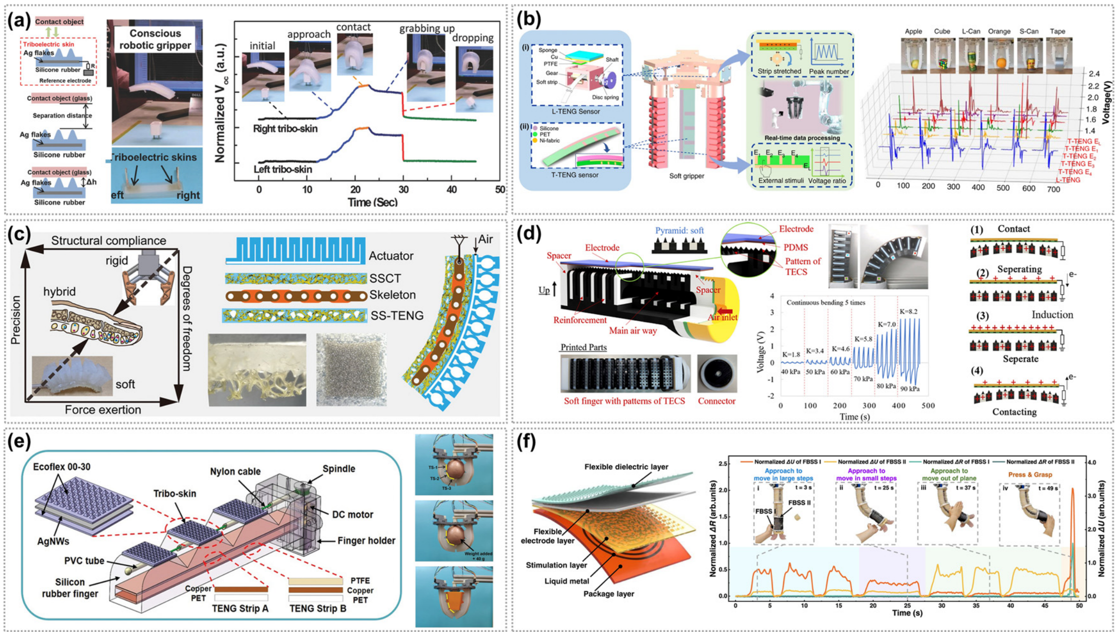

Fig. 8. Application of nanogenerator in soft robot. (a) TENG-based flexible sensor to detect movements of moving objects [130]. Copyright (2023) by John Wiley and Sons. (b) Smart soft-robotic gripper system based on TENG to detect various aspects of external stimuli [131]. Copyright (2023) by John Wiley and Sons. (c) Conductive sponge/porous silicone-based triboelectric nanogenerator (SS-TENG) for soft actuator to distinguish different objects [132]. Copyright (2023) by Elsevier. (d) Soft robotic finger featured a triboelectric curvature sensor using multi-material 3D printing technology [133]. Copyright (2023) by John Wiley and Sons. (e) Smart soft actuator with two types of TENGs to detect contact pressure and bending motion [134]. Copyright (2022) by Springer Nature. (f) Flexible bimodal smart skin (FBSS) using TENG and liquid metal sensing for touchless interactive teaching [135]. Copyright (2023) by Elsevier. (For interpretation of the references to color in this figure legend, the reader is referred to the web version of this article.)

transferred charge and open-circuit voltage. The direct quantization and intuitionistic mapping at the sensing stage greatly simplifies the signal processing and classification algorithms.

The rotary type of TENG has unique advantages in measuring angle displacement, as more stable performance and higher precision. In 2020, Wang et al. proposed a novel rotating grating-structured self-powered angle sensor (SPAS) that can be applied to robotic arms for recording the flexion and extension of joints (Fig. 7c) [124]. The device consisted of a rotator (two groups of freestanding electrodes) and a stator (Kapton electrification layer and two groups of interdigital electrodes) coaxially assembled, exhibiting the highest resolution (2.03 nano-radian). Similarly, in 2022, Qiao et al. proposed a distributed vector motion sensor based on dual-mode TENG as shown in Fig. 7d [121], which could simultaneously generate AC signal to monitor displacement or angle parameters and DC signal to directly judge movement direction, and the angle accuracy of the device reached 0.05° (1.7 μm).

However, contact-based sensing can easily cause rapid wear and tear of the device, which has certain limitations in long-term use scenarios. So that non-contact sensors are receiving increasing attention from researchers. In 2020, Wang et al. proposed a single-piece self-powered non-contact sensor with an interdigital sensitive layer capable of rotational movement detecting (Fig. 7e) [125]. Polyurethane (PU) and PTFE film were utilized for perceiving the rotation. Although this non-contact sensor had a longer lifespan, it fell short in accuracy compared to several previous works.

Besides, to enhance the sensor's versatility and enable it to detect inputs from multiple axes, in 2018, Koh et al. proposed a 3D activity inertial sensor (3DAIS) that incorporated hybrid energy harvesting mechanisms as electromagnetic, piezoelectric, and triboelectric technologies to enable 6-axis inertial sensing (Fig. 7f) [126]. This device boasted exceptional advantages when it came to detecting multi-axis acceleration and rotational inertia for use in robots.

Using 3D printing technology, in 2023, Wang et al. fabricated CNF/MXene-based deep-trap hierarchical architecture for high-performance TENG (Fig. 7g) [127]. The addition of MXene nanosheets to the printed scaffold resulted in a higher number of open pores, which enhanced charge generation of the device, thus better promoting the sensitivity of non-contact distance detection.

4. Application of nanogenerator in soft robots

Soft robots, which draw inspiration from the structure and motion of biological organisms, are an emerging type of robot. To enable intelligent control and behavior planning, these robots heavily rely on sensors that can measure the external environment and the robot's own state. By processing this information, soft robots are able to move efficiently, manipulate objects with precision, interact with their surroundings, and adapt to new situations with greater flexibility [128].

Flexible tactile sensors, for example, are particularly useful for soft robots as they can detect obstacles in the environment and enable the robot to avoid them with accuracy [129]. Thus, the robot can perform complex tasks and operations that require spatial awareness and agility. Therefore, the integration of sensors into soft robots is crucial for their intelligence and autonomy. The key to developing practical autonomous soft systems that have the ability to function over extended periods of time without electrical connections is their ability to operate with minimal power consumption. In this section, we will overview the current state of the art in nanogenerator devices that are used as flexible self-powered sensors for soft robots.

TENG-based sensors are particularly suitable for soft robots because the Young's modulus of the soft materials typically used in triboelectric sensors is similar to that of soft robots. In 2018, Lai et al. utilized a percolating silver-flake network as an extendable conductor and used super-soft yet tough Eco-flex 00–30 silicone rubbers for the encapsulated and triboelectric materials, as well as pneumatic actuators (Fig. 8a) [130]. The sensor allowed flexible robotic hand to be actively aware of different movements of moving objects, including approaching, grabbing, lifting, lowering, and even accidentally falling objects. In 2020, Jin

Fig. 9. Application of nanogenerator in HMI. (a) Cutting-edge smart glove with triboelectric tactile sensors and a PZT piezoelectric haptic mechanical stimulator [138]. Copyright (2020) by AAAS. (b) Sign language recognition and communication system comprising 15 triboelectric sensors integrated glove [139]. Copyright (2021) by Springer Nature. (c) Smart glove with simple-structured TENG for robotic hand controlling [140]. Copyright (2023) by Elsevier. (d) Self-powered visual tactile sensor to convert touch stimuli into visible light signals [141]. Copyright (2023) by John Wiley and Sons. (e) Textile-based multifunctional bracelet with triboelectric and piezoresistive sensors for robotic hand controlling [142]. Copyright (2023) by Elsevier. (f) Self-powered, flexible, triboelectric sensor (SFTS) patch for finger trajectory recording [143]. Copyright (2018) by American Chemical Society. (For interpretation of the references to color in this figure legend, the reader is referred to the web version of this article.)

et al. reported a smart soft-robotic gripper system based on triboelectric nanogenerator sensors (Fig. 8b) [131]. The T-TENG sensor, featuring patterned electrodes, was capable of sensing various aspects of external stimuli such as sliding, contact position and contact area through the triboelectric output generated by grating electrode. And the L-TENG sensor allowed for scalable measurement of bending motion.

The integrated sensors enable soft robotics to actively perceive and sense their deformation or response in real-time. In 2019, Chen et al. demonstrated a conductive sponge/porous silicone-based triboelectric nanogenerator (SS-TENG) for soft actuator, which could distinguish between different objects (Fig. 8c) [132]. With multi-material 3D printing, both the soft actuator and its functional sensor can be fabricated, facilitating a straightforward and efficient manufacturing process for controllable soft robotics. In 2020, Zhu et al. developed a soft robotic finger that featured a triboelectric curvature sensor (S-TECS) using multi-material 3D printing technology with stretchable electrodes (Fig. 8d) [133]. The integrated S-TECS which achieve fast prototyping and easy system integration can measure a finger curvature up to 8.2 m^{-1} under an ultra-low working frequency of 0.06 Hz. In 2020, Chen et al. proposed a smart soft actuator with tribo-skins through the integration of soft elastomers, cable-driven mechanism and TENGs, that the soft actuator integrated with two types of TENGs: a single-electrode-mode TENG to measure the contact pressure and an inner contact–separation-mode TENG to detect the bending motion (Fig. 8e) [134].

The triboelectric electronic skin's exceptional flexibility and sensitivity endowed the soft robot with the ability to sense and interact with its environment. Moreover, leveraging the advantage of this principle made it possible to achieve non-contact sensing in the robotic arm. In 2022, Liu et al. developed a flexible bimodal smart skin (FBSS) that can perform simultaneous tactile and touchless sensing using a TENG and liquid metal sensing (Fig. 8f) [135]. The structure of the device contained five flexible layers, that the surfaces of the flexible dielectric layer (PDMS with pyramid-shaped microstructures), flexible electrode layer (Ag nanowire networks), and stimulation layer (PDMS) formed chemical bonds after being treated with plasma. The soft robots with FBSS could enable complex movement through a touchless interactive teaching method, which had broad potential applications in the field of non-contact HMI.

5. Application of nanogenerator in HMI

The research on HMI systems can be traced back to the 1980s and has received increasing attention from researchers [136]. It is a highly interdisciplinary field, where sensors of different functions play a crucial role in the interaction between humans and robots. Based on sensor technology, robots can perceive various information such as human actions, sounds, and behaviors, providing corresponding feedback and responses, thus achieving a more natural and intelligent interaction process. For example, in virtual reality and augmented reality technologies, various sensors are used to achieve hand movement tracking, facial expression capture, and other functions, allowing users to experience a more immersive and realistic environment. In the industrial and medi-

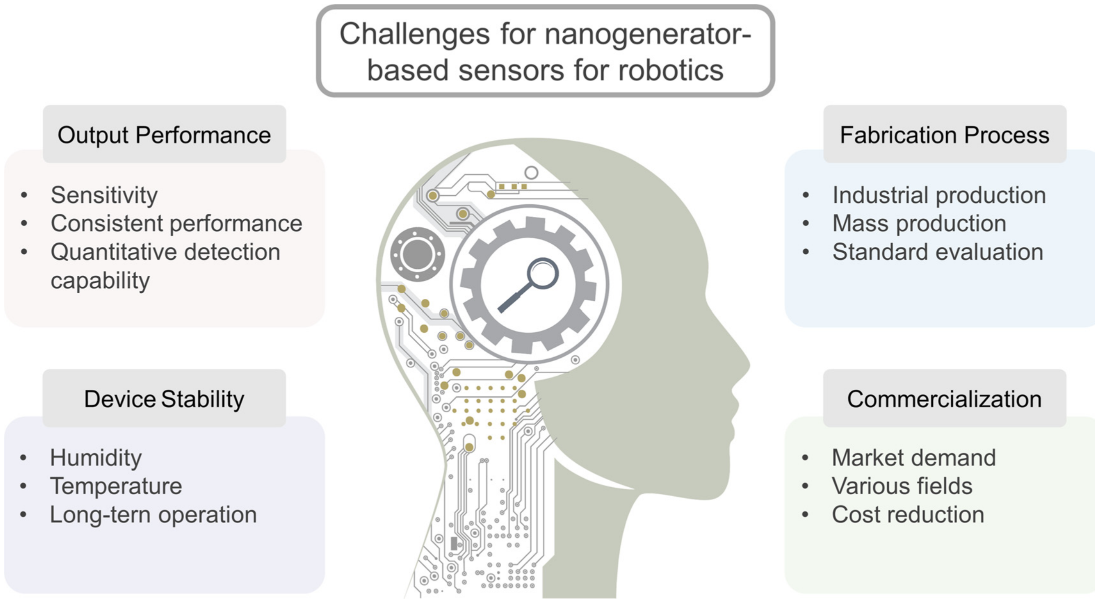

Fig. 10. Challenges for nanogenerator-based sensor in robotics.

cal fields, high-sensitivity sensors can be used to achieve precise control of mechanical arms. In recent years, nanogenerators have emerged as a promising alternative solution for efficient HMI [137]. In this chapter, we will introduce the latest research progress of nanogenerators in the field of HMI, mainly focusing on virtual reality and mechanical hand interaction.

In 2020, Zhu et al. designed a cutting-edge smart glove that incorporates elastomer-based triboelectric tactile sensors and a PZT piezoelectric haptic mechanical stimulator (Fig. 9a) [138]. The TENG-based sensor was capable of detecting the bending angle of human fingers and the normal force in eight directions of the palm. By combining with piezoelectric stimulator to achieve feedback interaction, it enabled more intuitive and bi-directional communication with virtual characters. In 2021, Wen et al. reported a sign language recognition and communication system comprising 15 triboelectric sensors integrated glove (Fig. 9b) [139]. Each thin triboelectric sensor consisted of ecoflex and wrinkled nitrile, and the conductive textile serves as electrodes. They also proposed a general semantic segmentation algorithm to improve the accuracy of sign language interaction, providing a dependable platform for effortless interaction between non-signers and signers with the gloves. In 2021, Luo et al. proposed a smart glove with simple-structured TENG using PDMS and silicon rubber for robotic hand controlling (Fig. 9c) [140]. The pressure visualization sensor can meet the application requirements of strength feedback and extended cross tactile perception, improving the efficiency of HMI. In 2022, Lu et al. reported a self-powered visual tactile sensor as shown in Fig. 9d [141], which consisted of a high-output TENG and a visual light source, that could convert touch stimuli into visible light signals (9.6 cd m^{-2}). The friction layer of TENG consists of chitosan and fluorinated ethylene propylene (FEP). They improved the friction area of the TENG by combining origami technology and surface engineering, and enhanced the charge transfer ability of the two materials by customizing the surface topography of the chitosan, which effectively enhanced the driving capability of the device (output power density 2.1 W m^{-2}).

The sensors mentioned above were carried by gloves. Some researchers have integrated the sensors into bracelets or attached them to the arm to facilitate HMI. In 2022, Pang et al. reported a textile-based multifunctional tactile sensor through the integration of triboelectric and piezoresistive sensors (Fig. 9e) [142]. Piezoresistive part utilized CNT-textile showed a high sensitivity of 11.2 kPa^{-1}, and TENG component made from Teflon-steel yarn stitched onto a cotton fabric successfully mimic the function of human FA mechanoreceptors, realizing the synchronous control of the robot. In 2018, Chen et al. presented a self-powered, flexible, triboelectric sensor (SFTS) patch for finger trajectory sensing, including a two-dimensional (2D) SFTS for in-plane robotic movement control and a one-dimensional (1D) SFTS for out-of-plane robotic movement control (Fig. 9f) [143]. The flexible substrate was made of silicone rubber, and the electrodes at the edge of the substrate were made of starch-based hydrogel PDMS elastomer (HPE). The combination of the 1D SFTS and 2D SFTS could achieve 3D motion control of a robotic manipulator (Fig. 10).

6. Conclusions and perspectives

This review provides a systematic summary of recent advancements in the development of nanogenerator-based sensors for use in robotics, including tactile sensing, auditory sensing, olfactory sensing, visual sensing and vector motion sensing. These developments have mainly been achieved through the exploration of new materials and optimization of functional structures. TENG based nanogenerators enable flexible tactile sensing/electronic skin to have various tactile perception abilities like pressure, shear force, slip, temperature, and even material identification due to its unique working principle. By designing the structure or processing the surface of the material, the selectivity of the device for frequency can be enhanced, which is of great significance for auditory perception applications. Some materials' sensitivity to gasses has broadened its application in olfactory perception. Moreover, the combination of flexible nanogenerators based on flexible materials and flexible mechanical hands can improve machine system performance and work efficiency, and also demonstrate unique advantages in human-machine interaction. In comparison, TENG has a wider range of material options, and the four working modes have expanded the range of its applications. PENG requires piezoelectric materials for charge induction, but it can produce stable output with less environmental interference. These two types of nanogenerators each have their own characteristics, and selecting the appropriate sensor based on their respective principles is crucial for getting maximum benefits in different scenarios.

Although nanogenerator-based sensors possess exceptional qualities, they continue to face numerous limitations that impede their practical implementation in robotics.

Output performance: Most of self-powered pressure sensors are only used for qualitative detection and lack accurate quantitative detection capabilities. For precise quantitative measurements of pressure, reliable calibration systems may need to be introduced in the future. Furthermore, the performance of self-powered skin sensors, including their sensitivity, must be further improved through material modification or structural design.

Device stability: The durability of sensors under harsh conditions, such as high temperature or high humidity environments, needs to be addressed to ensure optimal device reliability. These attributes should be considered essential features rather than add-ons. Future research must focus on improving these features to ensure that nanogenerator-based sensor can still perform optimally under harsh usage conditions.

Fabrication process: Current reports on nanogenerator sensor devices mainly use manual assembly technology, with a lack of exploration in large-area automatic production, which is crucial for maintaining consistency and stability of sensor performance.

Commercialization: Moreover, promoting the commercialization of nanogenerator sensing systems is also crucial, although this process is still in its infancy. Despite these challenges, it is encouraging that researchers have achieved exciting results over the past dozen years. It can be predicted that with the rapid development of materials and electronic technologies, self-powered sensors will have a promising future and will be more advanced in robotics applications.

Declaration of Competing Interest

The authors declare that they have no known competing financial interests or personal relationships that could have appeared to influence the work reported in this paper.

CRediT authorship contribution statement

Xuecheng Qu: Writing – original draft. **Ze Yang:** Visualization. **Jia Cheng:** Writing – review & editing, Supervision, Investigation. **Zhou Li:** Writing – review & editing, Supervision, Investigation. **Linhong Ji:** Writing – review & editing, Supervision, Investigation, Conceptualization.

Acknowledgments

This research was supported by National Key Research and Development Program of China (No. 2022YFB3804703, No. 2022YFB3804704, No. 2021YFB3200300), National Natural Science Foundation of China (No. 52075286).

References

[1] F. Tao, F.Y. Sui, A. Liu, Q.L. Qi, M. Zhang, B.Y. Song, Z.R. Guo, S.C.Y. Lu, A.Y.C. Nee, Digital twin-driven product design framework, Int. J. Prod. Res. 57 (2019) 3935–3953, doi:10.1080/00207543.2018.1443229.

[2] P.P.L. Regtien, Sensors for applications in robotics, Sens. Actuators 10 (1986) 195–218, doi:10.1016/0250-6874(86)80046-4.

[3] J.H. Ryu, M. Irfan, A. Reyaz, A review on sensor network issues and robotics, J. Sens. 2015 (2015) 140217, doi:10.1155/2015/140217.

[4] S. Liu, Y. Li, W. Guo, X. Huang, L. Xu, Y.-C. Lai, C. Zhang, H. Wu, Triboelectric nanogenerators enabled sensing and actuation for robotics, Nano Energy 65 (2019) 104005, doi:10.1016/j.nanoen.2019.104005.

[5] Y.S. Narang, J.J. Vlassak, R.D. Howe, Mechanically versatile soft machines through laminar jamming, Adv. Funct. Mater. 28 (2018) 1707136, doi:10.1002/adfm.201707136.

[6] R.S. Dahiya, P. Mittendorfer, M. Valle, G. Cheng, V.J. Lumelsky, Directions toward effective utilization of tactile skin: a review, IEEE Sens. J. 13 (2013) 4121–4138, doi:10.1109/JSEN.2013.2279056.

[7] H. Wang, M. Totaro, L. Beccai, Toward perceptive soft robots: progress and challenges, Adv. Sci. 5 (2018) 1800541, doi:10.1002/advs.201800541.

[8] Y. Liu, K. He, G. Chen, W.R. Leow, X. Chen, Nature-inspired structural materials for flexible electronic devices, Chem. Rev. 117 (2017) 12893–12941, doi:10.1021/acs.chemrev.7b00291.

[9] G.J. Lee, C. Choi, D.-H. Kim, Y.M. Song, Bioinspired artificial eyes: optic components, digital cameras, and visual prostheses, Adv. Funct. Mater. 28 (2018) 1705202, doi:10.1002/adfm.201705202.

[10] Y.M. Song, Y. Xie, V. Malyarchuk, J. Xiao, I. Jung, K.-J. Choi, Z. Liu, H. Park, C. Lu, R.-H. Kim, R. Li, K.B. Crozier, Y. Huang, J.A. Rogers, Digital cameras with designs inspired by the arthropod eye, Nature 497 (2013) 95–99, doi:10.1038/nature12083.

[11] Y.H. Jung, B. Park, J.U. Kim, T.-i. Kim, Bioinspired electronics for artificial sensory systems, Adv. Mater. 31 (2019) 1803637, doi:10.1002/adma.201803637.

[12] A. Chortos, Z. Bao, Skin-inspired electronic devices, Mater. Today 17 (2014) 321–331, doi:10.1016/j.mattod.2014.05.006.

[13] J. Park, M. Kim, Y. Lee, H.S. Lee, H. Ko, Fingertip skin–inspired microstructured ferroelectric skins discriminate static/dynamic pressure and temperature stimuli, Sci. Adv. 1 (2015) e1500661, doi:10.1126/sciadv.1500661.

[14] Q. Hua, J. Sun, H. Liu, R. Bao, R. Yu, J. Zhai, C. Pan, Z.L. Wang, Skin-inspired highly stretchable and conformable matrix networks for multifunctional sensing, Nat. Commun. 9 (2018) 244, doi:10.1038/s41467-017-02685-9.

[15] D. Kang, P.V. Pikhitsa, Y.W. Choi, C. Lee, S.S. Shin, L. Piao, B. Park, K.Y. Suh, T.I. Kim, M. Choi, Ultrasensitive mechanical crack-based sensor inspired by the spider sensory system, Nature 516 (2014) 222–226, doi:10.1038/nature14002.

[16] H. Zhao, K. O'Brien, S. Li, R.F. Shepherd, Optoelectronically innervated soft prosthetic hand via stretchable optical waveguides, Sci. Robot. 1 (2016) aai7529, doi:10.1126/scirobotics.aai7529.

[17] F.-X. Wang, M.-J. Wang, H.-C. Liu, Y.-L. Zhang, Q.-H. Lin, T. Chen, L.-N. Sun, Multifunctional self-powered E-skin with tactile sensing and visual warning for detecting robot safety, Adv. Mater. Interfaces 7 (2020) 2000536, doi:10.1002/admi.202000536.

[18] Z. Wang, T. Bu, Y. Li, D. Wei, B. Tao, Z. Yin, C. Zhang, H. Wu, Multidimensional force sensors based on triboelectric nanogenerators for electronic skin, ACS Appl. Mater. Interfaces 13 (2021) 56320–56328, doi:10.1021/acsami.1c17506.

[19] W. Zhang, Y. Xi, E. Wang, X. Qu, Y. Yang, Y. Fan, B. Shi, Z. Li, Self-powered force sensors for multidimensional tactile sensing, ACS Appl. Mater. Interfaces 14 (2022) 20122–20131, doi:10.1021/acsami.2c03812.

[20] X. Qu, J. Xue, Y. Liu, W. Rao, Z. Liu, Z. Li, Fingerprint-shaped triboelectric tactile sensor, Nano Energy 98 (2022) 107324, doi:10.1016/j.nanoen.2022.107324.

[21] X.D. Wang, L. Dong, H.L. Zhang, R.M. Yu, C.F. Pan, Z.L. Wang, Recent progress in electronic skin, Adv. Sci. 2 (2015) 1500169, doi:10.1002/advs.201500169.

[22] W. Zhou, C. Zhang, A. Ren, H. Dong, J. Yao, Y.S. Zhao, Responsive liquid-crystal microlaser arrays with tactile perception, Adv. Opt. Mater. (2023) 2202879, doi:10.1002/adom.202202879.

[23] I. You, S.E. Choi, H. Hwang, S.W. Han, J.W. Kim, U. Jeong, E-Skin tactile sensor matrix pixelated by position-registered conductive microparticles creating pressure-sensitive selectors, Adv. Funct. Mater. 28 (2018) 1801858, doi:10.1002/adfm.201801858.

[24] J.H. Lee, J.S. Heo, Y.J. Kim, J. Eom, H.J. Jung, J.W. Kim, I. Kim, H.H. Park, H.S. Mo, Y.H. Kim, S.K. Park, A behavior-learned cross-reactive sensor matrix for intelligent skin perception, Adv. Mater. 32 (2020) 2000969, doi:10.1002/adma.202000969.

[25] S. Pyo, J. Lee, K. Bae, S. Sim, J. Kim, Recent progress in flexible tactile sensors for human-interactive systems: from sensors to advanced applications, Adv. Mater. 33 (2021) 2005902, doi:10.1002/adma.202005902.

[26] K.I. Jang, H.U. Chung, S. Xu, C.H. Lee, H. Luan, J. Jeong, H. Cheng, G.T. Kim, S.Y. Han, J.W. Lee, J. Kim, M. Cho, F. Miao, Y. Yang, H.N. Jung, M. Flavin, H. Liu, G.W. Kong, K.J. Yu, S.I. Rhee, J. Chung, B. Kim, J.W. Kwak, M.H. Yun, J.Y. Kim, Y.M. Song, U. Paik, Y. Zhang, Y. Huang, J.A. Rogers, Soft network composite materials with deterministic and bio-inspired designs, Nat. Commun. 6 (2015) 6566, doi:10.1038/ncomms7566.

[27] M. Bachman, F.G. Zeng, T. Xu, G.P. Li, Micromechanical resonator array for an implantable bionic ear, Audiol. Neuro-otol. 11 (2006) 95–103, doi:10.1159/000090682.

[28] S. Kim, W.J. Song, J. Jang, J. Jang, H. Choi, Mechanical frequency selectivity of an artificial basilar membrane using a beam array with narrow supports, J. Micromech. Microeng. 23 (2013) 095018, doi:10.1088/0960-1317/23/9/095018.

[29] H.J. Jin, S.H. Lee, T.H. Kim, J. Park, H.S. Song, T.H. Park, S. Hong, Nanovesicle-based bioelectronic nose platform mimicking human olfactory signal transduction, Biosens. Bioelectron. 35 (2012) 335–341, doi:10.1016/j.bios.2012.03.012.

[30] S.H. Lee, O.S. Kwon, H.S. Song, S.J. Park, J.H. Sung, J. Jang, T.H. Park, Mimicking the human smell sensing mechanism with an artificial nose platform, Biomaterails 33 (2012) 1722–1729, doi:10.1016/j.biomaterials.2011.11.044.

[31] H. Yu, X. He, W. Ding, Y. Hu, D. Yang, S. Lu, C. Wu, H. Zou, R. Liu, C. Lu, Z.L. Wang, A self-powered dynamic displacement monitoring system based on triboelectric accelerometer, Adv. Energy Mater. 7 (2017) 1700565, doi:10.1002/aenm.201700565.

[32] J. Cao, X. Fu, H. Zhu, Z. Qu, Y. Qi, Z. Zhang, Z. Zhang, G. Cheng, C. Zhang, J. Ding, Self-powered non-contact motion vector sensor for multifunctional human–machine interface, Small Methods 6 (2022) 2200588, doi:10.1002/smtd.202200588.

[33] W. Hou, X. Tang, L. Fang, Q. Zheng, X. Chen, L. Zheng, Self-driven real-time angle vector sensor as security dialer based on bi-directional backstop triboelectric nanogenerator, Nano Energy 99 (2022) 107430, doi:10.1016/j.nanoen.2022.107430.

[34] B. Zhang, L. Zhang, W. Deng, L. Jin, F. Chun, H. Pan, B. Gu, H. Zhang, Z. Lv, W. Yang, Z.L. Wang, Self-powered acceleration sensor based on liquid metal triboelectric nanogenerator for vibration monitoring, ACS Nano 11 (2017) 7440–7446, doi:10.1021/acsnano.7b03818.

[35] H. Zhang, Y. Yang, Y. Su, J. Chen, K. Adams, S. Lee, C. Hu, Z.L. Wang, Triboelectric nanogenerator for harvesting vibration energy in full space and as self-powered acceleration sensor, Adv. Funct. Mater. 24 (2014) 1401–1407, doi:10.1002/adfm.201302453.

[36] W. Ding, A.C. Wang, C. Wu, H. Guo, Z.L. Wang, Human–machine interfacing enabled by triboelectric nanogenerators and tribotronics, Adv. Mater. Technol. 4 (2019) 1800487, doi:10.1002/admt.201800487.

[37] K.W. Cho, S.H. Sunwoo, Y.J. Hong, J.H. Koo, J.H. Kim, S. Baik, T. Hyeon, D.H. Kim, Soft bioelectronics based on nanomaterials, Chem. Rev. 122 (2022) 5068–5143, doi:10.1021/acs.chemrev.1c00531.

[38] F. Wen, C. Wang, C. Lee, Progress in self-powered sensors—Moving toward artificial intelligent and neuromorphic system, Nano Res. (2023) accepted, doi:10.1007/s12274-023-5879-4.
[39] Z. Sun, M. Zhu, C. Lee, Progress in the triboelectric human–machine interfaces (HMIs)-moving from smart gloves to AI/Haptic enabled HMI in the 5 G/IoT Era, Nanoenergy Adv. 1 (2021) 81–120, doi:10.3390/nanoenergyadv1010005.
[40] Y. Yang, X. Guo, M. Zhu, Z. Sun, Z. Zhang, T. He, C. Lee, Triboelectric nanogenerator enabled wearable sensors and electronics for sustainable internet of things integrated green earth, Adv. Energy Mater. 13 (2023) 2203040, doi:10.1002/aenm.202203040.
[41] M. Zhu, T. He, C. Lee, Technologies toward next generation human machine interfaces: from machine learning enhanced tactile sensing to neuromorphic sensory systems, Appl. Phys. Rev. 7 (2020) 031305, doi:10.1063/5.0016485.
[42] C.M. Boutry, M. Negre, M. Jorda, O. Vardoulis, A. Chortos, O. Khatib, Z. Bao, A hierarchically patterned, bioinspired e-skin able to detect the direction of applied pressure for robotics, Sci. Robot. 3 (2018), doi:10.1126/scirobotics.aau6914.
[43] S. Pyo, J. Lee, W. Kim, E. Jo, J. Kim, Multi-layered, hierarchical fabric-based tactile sensors with high sensitivity and linearity in ultrawide pressure range, Adv. Funct. Mater. 29 (2019) 1902484, doi:10.1002/adfm.201902484.
[44] X. Yu, Z. Xie, Y. Yu, J. Lee, A. Vazquez-Guardado, H. Luan, J. Ruban, X. Ning, A. Akhtar, D. Li, B. Ji, Y. Liu, R. Sun, J. Cao, Q. Huo, Y. Zhong, C. Lee, S. Kim, P. Gutruf, C. Zhang, Y. Xue, Q. Guo, A. Chempakasseril, P. Tian, W. Lu, J. Jeong, Y. Yu, J. Cornman, C. Tan, B. Kim, K. Lee, X. Feng, Y. Huang, J.A. Rogers, Skin-integrated wireless haptic interfaces for virtual and augmented reality, Nature 575 (2019) 473–479, doi:10.1038/s41586-019-1687-0.
[45] M. Dargusch, W.D. Liu, Z.G. Chen, Thermoelectric generators: alternative power supply for wearable electrocardiographic systems, Adv. Sci. 7 (2020) 2001362, doi:10.1002/advs.202001362.
[46] Z. Han, P. Jiao, Z. Zhu, Combination of piezoelectric and triboelectric devices for robotic self-powered sensors, Micromachines (Basel) 12 (2021) 813–814, doi:10.3390/mi12070813.
[47] C. Zhang, W. Tang, C. Han, F. Fan, Z.L. Wang, Theoretical comparison, equivalent transformation, and conjunction operations of electromagnetic induction generator and triboelectric nanogenerator for harvesting mechanical energy, Adv. Mater. 26 (2014) 3580–3591, doi:10.1002/adma.201400207.
[48] Z.L. Wang, J. Song, Piezoelectric nanogenerators based on zinc oxide nanowire arrays, Science 312 (2006) 242–246, doi:10.1126/science.1124005.
[49] F.-R. Fan, Z.-Q. Tian, Z.L. Wang, Flexible triboelectric generator, Nano Energy 1 (2012) 328–334, doi:10.1016/j.nanoen.2012.01.004.
[50] Y. Cao, Y. Yang, X. Qu, B. Shi, L. Xu, J. Xue, C. Wang, Y. Bai, Y. Gai, D. Luo, Z. Li, A self-powered triboelectric hybrid coder for human–machine interaction, Small Methods 6 (2022) 2101529, doi:10.1002/smtd.202101529.
[51] Z. Liu, L. Xu, Q. Zheng, Y. Kang, B. Shi, D. Jiang, H. Li, X. Qu, Y. Fan, Z.L. Wang, Z. Li, Human motion driven self-powered photodynamic system for long-term autonomous cancer therapy, ACS Nano 14 (2020) 8074–8083, doi:10.1021/acsnano.0c00675.
[52] Z. Liu, Y. Zhou, X. Qu, L. Xu, Y. Zou, Y. Shan, J. Shao, C. Wang, Y. Liu, J. Xue, D. Jiang, Y. Fan, Z. Li, H. Ye, A self-powered optogenetic system for implantable blood glucose control, Research (2022), doi:10.34133/2022/9864734.
[53] F. Mokhtari, J. Foroughi, T. Zheng, Z. Cheng, G.M. Spinks, Triaxial braided piezo fiber energy harvesters for self-powered wearable technologies, J. Mater. Chem. A 7 (2019) 8245–8257, doi:10.1039/C8TA10964H.
[54] S. Mondal, T. Paul, S. Maiti, B.K. Das, K.K. Chattopadhyay, Human motion interactive mechanical energy harvester based on all inorganic perovskite-PVDF, Nano Energy 74 (2020) 104870, doi:10.1016/j.nanoen.2020.104870.
[55] H. Ouyang, Z. Liu, N. Li, B. Shi, Y. Zou, F. Xie, Y. Ma, Z. Li, H. Li, Q. Zheng, X. Qu, Y. Fan, Z.L. Wang, H. Zhang, Z. Li, Symbiotic cardiac pacemaker, Nat. Commun. 10 (2019) 1821, doi:10.1038/s41467-019-09851-1.
[56] X. Qu, Y. Liu, Z. Liu, Z. Li, Assistive devices for the people with disabilities enabled by triboelectric nanogenerators, J. Phys. 4 (2021) 034015, doi:10.1088/2515-7639/ac0092.
[57] X. Qu, X. Ma, B. Shi, H. Li, L. Zheng, C. Wang, Z. Liu, Y. Fan, X. Chen, Z. Li, Z.L. Wang, Refreshable braille display system based on triboelectric nanogenerator and dielectric elastomer, Adv. Funct. Mater. 31 (2021) 2006612, doi:10.1002/adfm.202006612.
[58] B. Shi, Z. Liu, Q. Zheng, J. Meng, H. Ouyang, Y. Zou, D. Jiang, X. Qu, M. Yu, L. Zhao, Y. Fan, Z.L. Wang, Z. Li, Body-integrated self-powered system for wearable and implantable applications, ACS Nano 13 (2019) 6017–6024, doi:10.1021/acsnano.9b02233.
[59] P. Tan, X. Han, Y. Zou, X. Qu, J. Xue, T. Li, Y. Wang, R. Luo, X. Cui, Y. Xi, L. Wu, B. Xue, D. Luo, Y. Fan, X. Chen, Z. Li, Z.L. Wang, Self-powered gesture recognition wristband enabled by machine learning for full keyboard and multicommand input, Adv. Mater. 34 (2022) 2200793, doi:10.1002/adma.202200793.
[60] C. Wang, X. Qu, Q. Zheng, Y. Liu, P. Tan, B. Shi, H. Ouyang, S. Chao, Y. Zou, C. Zhao, Z. Liu, Y. Li, Z. Li, Stretchable, self-healing, and skin-mounted active sensor for multipoint muscle function assessment, ACS Nano 15 (2021) 10130–10140, doi:10.1021/acsnano.1c02010.
[61] Y. Yang, L. Xu, D. Jiang, B.Z. Chen, R. Luo, Z. Liu, X. Qu, C. Wang, Y. Shan, Y. Cui, H. Zheng, Z. Wang, Z.L. Wang, X.D. Guo, Z. Li, Self-powered controllable transdermal drug delivery system, Adv. Funct. Mater. 31 (2021) 2104092, doi:10.1002/adfm.202104092.
[62] S.L. Zhang, C.G. Koh, K.S.C. Kuang, Proposed rail pad sensor for wheel-rail contact force monitoring, Smart Mater. Struct. 27 (2018) 115041, doi:10.1088/1361-665X/aadc8d.
[63] Q. Zheng, Y. Hou, H. Yang, P. Tan, H. Shi, Z. Xu, Z. Ye, N. Chen, X. Qu, X. Han, Y. Zou, X. Cui, H. Yao, Y. Chen, W. Yao, J. Zhang, Y. Chen, J. Liang, X. Gu, D. Wang, Y. Wei, J. Xue, B. Jing, Z. Zeng, L. Wang, Z. Li, Z.L. Wang, Towards a sustainable monitoring: a self-powered smart transportation infrastructure skin, Nano Energy 98 (2022) 107245, doi:10.1016/j.nanoen.2022.107245.
[64] Y. Zhou, J. He, H. Wang, K. Qi, N. Nan, X. You, W. Shao, L. Wang, B. Ding, S. Cui, Highly sensitive, self-powered and wearable electronic skin based on pressure-sensitive nanofiber woven fabric sensor, Sci. Rep. 7 (2017) 12949, doi:10.1038/s41598-017-13281-8.
[65] Y. Zou, Y. Gai, P. Tan, D. Jiang, X. Qu, J. Xue, H. Ouyang, B. Shi, L. Li, D. Luo, Y. Deng, Z. Li, Z.L. Wang, Stretchable graded multichannel self-powered respiratory sensor inspired by shark gill, Fundam. Res. 2 (2022) 619–628, doi:10.1016/j.fmre.2022.01.003.
[66] Y. Zou, P. Tan, B. Shi, H. Ouyang, D. Jiang, Z. Liu, H. Li, M. Yu, C. Wang, X. Qu, L. Zhao, Y. Fan, Z.L. Wang, Z. Li, A bionic stretchable nanogenerator for underwater sensing and energy harvesting, Nat. Commun. 10 (2019) 2695, doi:10.1038/s41467-019-10433-4.
[67] Z.-Y. Huo, D.-M. Lee, J.-M. Jeong, Y.-J. Kim, J. Kim, I.-Y. Suh, P. Xiong, S.-W. Kim, Microbial disinfection with supercoiling capacitive triboelectric nanogenerator, Adv. Energy Mater. 12 (2022) 2103680, doi:10.1002/aenm.202103680.
[68] G.-T. Hwang, H. Park, J.-H. Lee, S. Oh, K.-I. Park, M. Byun, H. Park, G. Ahn, C.K. Jeong, K. No, H. Kwon, S.-G. Lee, B. Joung, K.J. Lee, Self-powered cardiac pacemaker enabled by flexible single crystalline pmn-pt piezoelectric energy harvester, Adv. Mater. 26 (2014) 4880–4887, doi:10.1002/adma.201400562.
[69] D.M. Lee, N. Rubab, I. Hyun, W. Kang, Y.-J. Kim, M. Kang, B.O. Choi, S.-W. Kim, Ultrasound-mediated triboelectric nanogenerator for powering on-demand transient electronics, Sci. Adv. 8 eabl8423. doi:10.1126/sciadv.abl8423.
[70] W. Liu, Z. Wang, G. Wang, G. Liu, J. Chen, X. Pu, Y. Xi, X. Wang, H. Guo, C. Hu, Z.L. Wang, Integrated charge excitation triboelectric nanogenerator, Nat. Commun. 10 (2019) 1426, doi:10.1038/s41467-019-09464-8.
[71] Y. Long, J. Li, F. Yang, J. Wang, X. Wang, Wearable and implantable electroceuticals for therapeutic electrostimulations, Adv. Sci. 8 (2021) 2004023, doi:10.1002/advs.202004023.
[72] H. Ryu, H.-m. Park, M.-K. Kim, B. Kim, H.S. Myoung, T.Y. Kim, H.-J. Yoon, S.S. Kwak, J. Kim, T.H. Hwang, E.-K. Choi, S.-W. Kim, Self-rechargeable cardiac pacemaker system with triboelectric nanogenerators, Nat. Commun. 12 (2021) 4374, doi:10.1038/s41467-021-24417-w.
[73] Z. Liu, B. Tian, Y. Li, J. Lei, Z. Zhang, J. Liu, Q. Lin, C. Lee, Z. Jiang, A large-area bionic skin for high-temperature energy harvesting applications, Nano Res. (2023) accept., doi:10.1007/s12274-023-5699-6.
[74] Q. Shi, Z. Sun, X. Le, J. Xie, C. Lee, Soft robotic perception system with ultrasonic auto-positioning and multimodal sensory intelligence, ACS Nano 17 (2023) 4985–4998, doi:10.1021/acsnano.2c12592.
[75] C. Wang, Y. Hu, Y. Liu, Y. Shan, X. Qu, J. Xue, T. He, S. Cheng, H. Zhou, W. Liu, Z.H. Guo, W. Hua, Z. Liu, Z. Li, C. Lee, Tissue-adhesive piezoelectric soft sensor for in vivo blood pressure monitoring during surgical operation, Adv. Funct. Mater. (2023) 2303696, doi:10.1002/adfm.202303696.
[76] S. An, X. Pu, S. Zhou, Y. Wu, G. Li, P. Xing, Y. Zhang, C. Hu, Deep learning enabled neck motion detection using a triboelectric nanogenerator, ACS Nano 16 (2022) 9359–9367, doi:10.1021/acsnano.2c02149.
[77] K. Qin, C. Chen, X. Pu, Q. Tang, W. He, Y. Liu, Q. Zeng, G. Liu, H. Guo, C. Hu, Magnetic array assisted triboelectric nanogenerator sensor for real-time gesture interaction, Nano-Micro Lett. 13 (2021) 51, doi:10.1007/s40820-020-00575-2.
[78] X. Pu, Q. Tang, W. Chen, Z. Huang, G. Liu, Q. Zeng, J. Chen, H. Guo, L. Xin, C. Hu, Flexible triboelectric 3D touch pad with unit subdivision structure for effective XY positioning and pressure sensing, Nano Energy 76 (2020) 105047, doi:10.1016/j.nanoen.2020.105047.
[79] Z.L. Wang, Triboelectric nanogenerators as new energy technology and self-powered sensors – Principles, problems and perspectives, Faraday Discuss. 176 (2014) 447–458, doi:10.1039/C4FD00159A.
[80] Z.L. Wang, On Maxwell's displacement current for energy and sensors: the origin of nanogenerators, Mater. Today 20 (2017) 74–82, doi:10.1016/j.mattod.2016.12.001.
[81] M. Ma, Z. Kang, Q. Liao, Q. Zhang, F. Gao, X. Zhao, Z. Zhang, Y. Zhang, Development, applications, and future directions of triboelectric nanogenerators, Nano Res. 11 (2018) 2951–2969, doi:10.1007/s12274-018-1997-9.
[82] C. Wu, A.C. Wang, W. Ding, H. Guo, Z.L. Wang, Triboelectric nanogenerator: a foundation of the energy for the new era, Adv. Energy Mater. 9 (2019) 1802906, doi:10.1002/aenm.201802906.
[83] J.B. Liseli, J. Agnus, P. Lutz, M. Rakotondrabe, An overview of piezoelectric self-sensing actuation for nanopositioning applications: electrical circuits, displacement, and force estimation, IEEE Trans. Instrum. Meas. 69 (2020) 2–14, doi:10.1109/TIM.2019.2950760.
[84] G.Y. Gu, L.M. Zhu, C.Y. Su, H. Ding, S. Fatikow, Modeling and control of piezo-actuated nanopositioning stages: a survey, IEEE Trans. Autom. Sci. Eng. 13 (2016) 313–332, doi:10.1109/TASE.2014.2352364.
[85] Y. Wang, P. Tan, Y. Wu, D. Luo, Z. Li, Artificial intelligence-enhanced skin-like sensors based on flexible nanogenerators, VIEW 3 (2022) 20220026, doi:10.1002/VIW.20220026.
[86] X. Wei, H. Li, W. Yue, S. Gao, Z. Chen, Y. Li, G. Shen, A high-accuracy, real-time, intelligent material perception system with a machine-learning-motivated pressure-sensitive electronic skin, Matter 5 (2022) 1481–1501, doi:10.1016/j.matt.2022.02.016.
[87] J.T. Nguyen, W. Cheng, A review on epidermal nanogenerators: recent progress of the future self-powered skins, Small Struct. 3 (2022) 2200034, doi:10.1002/sstr.202200034.

[88] C. Wang, R.-R. Bao, C.-F. Pan, Research and application of flexible wearable electronics based on nanogenerator in touch sensor, Acta. Physica. Sinica. 70 (2021) 100705–100715, doi:10.7498/aps.70.20202157.
[89] S. Chun, W. Son, H. Kim, S.K. Lim, C. Pang, C. Choi, Self-powered pressure- and vibration-sensitive tactile sensors for learning technique-based neural finger skin, Nano Lett. 19 (2019) 3305–3312, doi:10.1021/acs.nanolett.9b00922.
[90] S.-R. Kim, S. Lee, J.-W. Park, A skin-inspired, self-powered tactile sensor, Nano Energy 101 (2022) 107608, doi:10.1016/j.nanoen.2022.107608.
[91] C. Zhang, S. Liu, X. Huang, W. Guo, Y. Li, H. Wu, A stretchable dual-mode sensor array for multifunctional robotic electronic skin, Nano Energy 62 (2019) 164–170, doi:10.1016/j.nanoen.2019.05.046.
[92] M. Han, H. Wang, Y. Yang, C. Liang, W. Bai, Z. Yan, H. Li, Y. Xue, X. Wang, B. Akar, H. Zhao, H. Luan, J. Lim, I. Kandela, G.A. Ameer, Y. Zhang, Y. Huang, J.A. Rogers, Three-dimensional piezoelectric polymer microsystems for vibrational energy harvesting, robotic interfaces and biomedical implants, Nat. Electron. 2 (2019) 26–35, doi:10.1038/s41928-018-0189-7.
[93] J. Li, Y. Liu, M. Wu, K. Yao, Z. Gao, Y. Gao, X. Huang, T.H. Wong, J. Zhou, D. Li, H. Li, J. Li, Y. Huang, R. Shi, J. Yu, X. Yu, Thin, soft, 3D printing enabled crosstalk minimized triboelectric nanogenerator arrays for tactile sensing, Fundam. Res. 3 (2023) 111–117, doi:10.1016/j.fmre.2022.01.021.
[94] T. Bu, T. Xiao, Z. Yang, G. Liu, X. Fu, J. Nie, T. Guo, Y. Pang, J. Zhao, F. Xi, C. Zhang, Z.L. Wang, Stretchable triboelectric–photonic smart skin for tactile and gesture sensing, Adv. Mater. 30 (2018) 1800066, doi:10.1002/adma.201800066.
[95] X. Qu, Z. Liu, P. Tan, C. Wang, Y. Liu, H. Feng, D. Luo, Z. Li, Z.L. Wang, Artificial tactile perception smart finger for material identification based on triboelectric sensing, Sci. Adv. 8 (2022) eabq2521, doi:10.1126/sciadv.abq2521.
[96] H. Shintaku, T. Nakagawa, D. Kitagawa, H. Tanujaya, S. Kawano, J. Ito, Development of piezoelectric acoustic sensor with frequency selectivity for artificial cochlea, Sens. Actuators, A 158 (2010) 183–192, doi:10.1016/j.sna.2009.12.021.
[97] T. Inaoka, H. Shintaku, T. Nakagawa, S. Kawano, H. Ogita, T. Sakamoto, S. Hamanishi, H. Wada, J. Ito, Piezoelectric materials mimic the function of the cochlear sensory epithelium, Proc. Natl. Acad. Sci. 108 (2011) 18390–18395, doi:10.1073/pnas.1110036108.
[98] G.-T. Hwang, M. Byun, C.K. Jeong, K.J. Lee, Flexible piezoelectric thin-film energy harvesters and nanosensors for biomedical applications, Adv. Healthcare Mater. 4 (2015) 646, doi:10.1002/adhm.201400642.
[99] J.H. Han, J.-H. Kwak, D.J. Joe, S.K. Hong, H.S. Wang, J.H. Park, S. Hur, K.J. Lee, Basilar membrane-inspired self-powered acoustic sensor enabled by highly sensitive multi tunable frequency band, Nano Energy 53 (2018) 198–205, doi:10.1016/j.nanoen.2018.08.053.
[100] J. Jang, J. Lee, J.H. Jang, H. Choi, A triboelectric-based artificial basilar membrane to mimic cochlear tonotopy, Adv. Healthcare Mater. 5 (2016) 2481–2487, doi:10.1002/adhm.201600232.
[101] W. Li, D. Torres, R. Díaz, Z. Wang, C. Wu, C. Wang, Z.L. Wang, N. Sepúlveda, Nanogenerator-based dual-functional and self-powered thin patch loudspeaker or microphone for flexible electronics, Nat. Commun. 8 (2017) 15310, doi:10.1038/ncomms15310.
[102] L. Zhou, J. He, W. Li, P. He, Q. Ye, B. Fu, P. Tao, C. Song, J. Wu, T. Deng, W. Shang, Butterfly wing hears sound: acoustic detection using biophotonic nanostructure, Nano Lett. 19 (2019) 2627–2633, doi:10.1021/acs.nanolett.9b00468.
[103] H. Guo, X. Pu, J. Chen, Y. Meng, M.-H. Yeh, G. Liu, Q. Tang, B. Chen, D. Liu, S. Qi, C. Wu, C. Hu, J. Wang, Z.L. Wang, A highly sensitive, self-powered triboelectric auditory sensor for social robotics and hearing aids, Sci. Rob. 3 (2018) eaat2516, doi:10.1126/scirobotics.aat2516.
[104] J. Yang, J. Chen, Y. Su, Q. Jing, Z. Li, F. Yi, X. Wen, Z. Wang, Z.L. Wang, Eardrum-inspired active sensors for self-powered cardiovascular system characterization and throat-attached anti-interference voice recognition, Adv. Mater. 27 (2015) 1316–1326, doi:10.1002/adma.201404794.
[105] S.-Y. Yun, J.-K. Han, S.-W. Lee, J.-M. Yu, S.-B. Jeon, Y.-K. Choi, Self-aware artificial auditory neuron with a triboelectric sensor for spike-based neuromorphic hardware, Nano Energy 109 (2023) 108322, doi:10.1016/j.nanoen.2023.108322.
[106] Y. Liu, Y. Zhu, J. Liu, Y. Zhang, J. Liu, J. Zhai, Design of bionic cochlear basilar membrane acoustic sensor for frequency selectivity based on film triboelectric nanogenerator, Nanoscale Res. Lett. 13 (2018) 191, doi:10.1186/s11671-018-2593-3.
[107] J.H. Han, K.M. Bae, S.K. Hong, H. Park, J.-H. Kwak, H.S. Wang, D.J. Joe, J.H. Park, Y.H. Jung, S. Hur, C.D. Yoo, K.J. Lee, Machine learning-based self-powered acoustic sensor for speaker recognition, Nano Energy 53 (2018) 658–665, doi:10.1016/j.nanoen.2018.09.030.
[108] H.S. Lee, J. Chung, G.-T. Hwang, C.K. Jeong, Y. Jung, J.-H. Kwak, H. Kang, M. Byun, W.D. Kim, S. Hur, S.-H. Oh, K.J. Lee, Flexible inorganic piezoelectric acoustic nanosensors for biomimetic artificial hair cells, Adv. Funct. Mater. 24 (2014) 6914–6921, doi:10.1002/adfm.201402270.
[109] J. Park, D.H. Kang, H. Chae, S.K. Ghosh, C. Jeong, Y. Park, S. Cho, Y. Lee, J. Kim, Y. Ko, J.J. Kim, H. Ko, Frequency-selective acoustic and haptic smart skin for dual-mode dynamic/static human-machine interface, Sci. Adv. 8 (2022) eabj9220, doi:10.1126/sciadv.abj9220.
[110] D. Zhang, Z. Yang, P. Li, M. Pang, Q. Xue, Flexible self-powered high-performance ammonia sensor based on Au-decorated MoSe2 nanoflowers driven by single layer MoS2-flake piezoelectric nanogenerator, Nano Energy 65 (2019) 103974, doi:10.1016/j.nanoen.2019.103974.
[111] H. He, C. Dong, Y. Fu, W. Han, T. Zhao, L. Xing, X. Xue, Self-powered smelling electronic-skin based on the piezo-gas-sensor matrix for real-time monitoring the mining environment, Sens. Actuators, B 267 (2018) 392–402, doi:10.1016/j.snb.2018.04.046.
[112] C. Huang, G. Chen, A. Nashalian, J. Chen, Advances in self-powered chemical sensing via a triboelectric nanogenerator, Nanoscale 13 (2021) 2065–2081, doi:10.1039/D0NR07770D.
[113] J.-H. Kim, J. Chun, J.W. Kim, W.J. Choi, J.M. Baik, Self-powered, room-temperature electronic nose based on triboelectrification and heterogeneous catalytic reaction, Adv. Funct. Mater. 25 (2015) 7049–7055, doi:10.1002/adfm.201503419.
[114] T. Grzebyk, A. Górecka-Drzazga, MEMS type ionization vacuum sensor, Sens. Actuators, A 246 (2016) 148–155, doi:10.1016/j.sna.2016.05.021.
[115] J. Zhu, Z. Sun, J. Xu, R.D. Walczak, J.A. Dziuban, C. Lee, Volatile organic compounds sensing based on Bennet doubler-inspired triboelectric nanogenerator and machine learning-assisted ion mobility analysis, Sci. Bull. 66 (2021) 1176–1185, doi:10.1016/j.scib.2021.03.021.
[116] J. Chang, H. Meng, C. Li, J. Gao, S. Chen, Q. Hu, H. Li, L. Feng, A wearable toxic gas-monitoring device based on triboelectric nanogenerator for self-powered aniline early warning, Adv. Mater. Technol. 5 (2020) 1901087, doi:10.1002/admt.201901087.
[117] Z. Qu, Y. Fu, B. Yu, P. Deng, L. Xing, X. Xue, High and fast H2S response of NiO/ZnO nanowire nanogenerator as a self-powered gas sensor, Sens. Actuators, B 222 (2016) 78–86, doi:10.1016/j.snb.2015.08.058.
[118] J. Yu, X. Yang, G. Gao, Y. Xiong, Y. Wang, J. Han, Y. Chen, H. Zhang, Q. Sun, Z.L. Wang, Bioinspired mechano-photonic artificial synapse based on graphene/MoS2 heterostructure, Sci. Adv. 7 (2021) eabd9117, doi:10.1126/sciadv.abd9117.
[119] S. Li, Z. Zhao, D. Liu, J. An, Y. Gao, L. Zhou, Y. Li, S. Cui, J. Wang, Z.L. Wang, A self-powered dual-type signal vector sensor for smart robotics and automatic vehicles, Adv. Mater. 34 (2022) 2110363, doi:10.1002/adma.202110363.
[120] X. Yin, D. Liu, L. Zhou, X. Li, G. Xu, L. Liu, S. Li, C. Zhang, J. Wang, Z.L. Wang, A motion vector sensor via direct-current triboelectric nanogenerator, Adv. Funct. Mater. 30 (2020) 2002547, doi:10.1002/adfm.202002547.
[121] W. Qiao, L. Zhou, Z. Zhao, D. Liu, S. Li, J. An, X. Li, Y. Gao, P. Yang, J. Liu, Z.L. Wang, J. Wang, A self-powered vector motion sensor for smart robotics and personalized medical rehabilitation, Nano Energy 104 (2022) 107936, doi:10.1016/j.nanoen.2022.107936.
[122] X. Pu, H. Guo, Q. Tang, J. Chen, L. Feng, G. Liu, X. Wang, Y. Xi, C. Hu, Z.L. Wang, Rotation sensing and gesture control of a robot joint via triboelectric quantization sensor, Nano Energy 54 (2018) 453–460, doi:10.1016/j.nanoen.2018.10.044.
[123] S. Wang, M. He, B. Weng, L. Gan, Y. Zhao, N. Li, Y. Xie, Stretchable and wearable triboelectric nanogenerator based on kinesio tape for self-powered human motion sensing, Nanomaterials 8 (2018) 657–669, doi:10.3390/nano8090657.
[124] Z. Wang, J. An, J. Nie, J. Luo, J. Shao, T. Jiang, B. Chen, W. Tang, Z.L. Wang, A self-powered angle sensor at nanoradian-resolution for robotic arms and personalized medicare, Adv. Mater. 32 (2020) 2001466, doi:10.1002/adma.202001466.
[125] Z. Wang, F. Zhang, T. Yao, N. Li, X. Li, J. Shang, Self-powered non-contact triboelectric rotation sensor with interdigitated film, Sensors 20 (2020) 4947–4961, doi:10.3390/s20174947.
[126] K.H. Koh, Q. Shi, S. Cao, D. Ma, H.Y. Tan, Z. Guo, C. Lee, A self-powered 3D activity inertial sensor using hybrid sensing mechanisms, Nano Energy 56 (2019) 651–661, doi:10.1016/j.nanoen.2018.11.075.
[127] B. Wang, M. Gao, X. Fu, M. Geng, Y. Liu, N. Cheng, J. Li, L. Li, Z. Zhang, Y. Song, 3D printing deep-trap hierarchical architecture-based non-contact sensor for multi-direction motion monitoring, Nano Energy 107 (2023) 108135, doi:10.1016/j.nanoen.2022.108135.
[128] M. Pan, C. Yuan, X. Liang, J. Zou, Y. Zhang, C. Bowen, Triboelectric and piezoelectric nanogenerators for future soft robots and machines, iScience 23 (2020) 101682, doi:10.1016/j.isci.2020.101682.
[129] J. Chen, K. Han, J. Luo, L. Xu, W. Tang, Z.L. Wang, Soft robots with self-powered configurational sensing, Nano Energy 77 (2020) 105171, doi:10.1016/j.nanoen.2020.105171.
[130] Y.-C. Lai, J. Deng, R. Liu, Y.-C. Hsiao, S.L. Zhang, W. Peng, H.-M. Wu, X. Wang, Z.L. Wang, Actively perceiving and responsive soft robots enabled by self-powered, highly extensible, and highly sensitive triboelectric proximity- and pressure-sensing skins, Adv. Mater. 30 (2018) 1801114, doi:10.1002/adma.201801114.
[131] T. Jin, Z. Sun, L. Li, Q. Zhang, M. Zhu, Z. Zhang, G. Yuan, T. Chen, Y. Tian, X. Hou, C. Lee, Triboelectric nanogenerator sensors for soft robotics aiming at digital twin applications, Nat. Commun. 11 (2020) 5381, doi:10.1038/s41467-020-19059-3.
[132] J. Chen, B. Chen, K. Han, W. Tang, Z.L. Wang, A triboelectric nanogenerator as a self-powered sensor for a soft–rigid hybrid actuator, Adv. Mater. Technol. 4 (2019) 1900337, doi:10.1002/admt.201900337.
[133] M. Zhu, M. Xie, X. Lu, S. Okada, S. Kawamura, A soft robotic finger with self-powered triboelectric curvature sensor based on multi-material 3D printing, Nano Energy 73 (2020) 104772, doi:10.1016/j.nanoen.2020.104772.
[134] S. Chen, Y. Pang, H. Yuan, X. Tan, C. Cao, Smart soft actuators and grippers enabled by self-powered tribo-skins, Adv. Mater. Technol. 5 (2020) 1901075, doi:10.1002/admt.201901075.
[135] W. Liu, Y. Duo, J. Liu, F. Yuan, L. Li, L. Li, G. Wang, B. Chen, S. Wang, H. Yang, Y. Liu, Y. Mo, Y. Wang, B. Fang, F. Sun, X. Ding, C. Zhang, L. Wen, Touchless interactive teaching of soft robots through flexible bimodal sensory interfaces, Nat. Commun. 13 (2022) 5030, doi:10.1038/s41467-022-32702-5.
[136] J. Xue, Y. Zou, Y. Deng, Z. Li, Bioinspired sensor system for health care and human-machine interaction, EcoMat 4 (2022) e12209, doi:10.1002/eom2.12209.
[137] H. Zhou, W. Huang, Z. Xiao, S. Zhang, W. Li, J. Hu, T. Feng, J. Wu, P. Zhu, Y. Mao, Deep-learning-assisted noncontact gesture-recognition system for touchless human-machine interfaces, Adv. Funct. Mater. 32 (2022) 2208271, doi:10.1002/adfm.202208271.

[138] M. Zhu, Z. Sun, Z. Zhang, Q. Shi, T. He, H. Liu, T. Chen, C. Lee, Haptic-feedback smart glove as a creative human-machine interface (HMI) for virtual/augmented reality applications, Scii. Adv. 6 (2020) eaaz8693, doi:10.1126/sciadv.aaz8693.
[139] F. Wen, Z. Zhang, T. He, C. Lee, AI enabled sign language recognition and VR space bidirectional communication using triboelectric smart glove, Nat. Commun. 12 (2021) 5378, doi:10.1038/s41467-021-25637-w.
[140] Y. Luo, Z. Wang, J. Wang, X. Xiao, Q. Li, W. Ding, H.Y. Fu, Triboelectric bending sensor based smart glove towards intuitive multi-dimensional human-machine interfaces, Nano Energy 89 (2021) 106330, doi:10.1016/j.nanoen.2021.106330.
[141] D. Lu, T. Liu, X. Meng, B. Luo, J. Yuan, Y. Liu, S. Zhang, C. Cai, C. Gao, J. Wang, S. Wang, S. Nie, Wearable triboelectric visual sensors for tactile perception, Adv. Mater. 35 (2023) 2209117, doi:10.1002/adma.202209117.
[142] Y. Pang, X. Xu, S. Chen, Y. Fang, X. Shi, Y. Deng, Z.-L. Wang, C. Cao, Skin-inspired textile-based tactile sensors enable multifunctional sensing of wearables and soft robots, Nano Energy 96 (2022) 107137, doi:10.1016/j.nanoen.2022.107137.
[143] T. Chen, Q. Shi, M. Zhu, T. He, L. Sun, L. Yang, C. Lee, Triboelectric self-powered wearable flexible patch as 3D motion control interface for robotic manipulator, ACS Nano 12 (2018) 11561–11571, doi:10.1021/acsnano.8b06747.